

## **SnowEx 2021 Moccasin MT UAV LiDAR Report**

***Project Location:***  
**Town of Moccasin**  
**Judith Basin County, Montana**



### **Summary**

DJ&A, P.C. was contracted by Montana State University (MSU) Department of Earth Sciences to collect aerial LiDAR datasets using an unmanned aerial vehicle (UAV) for the 2021 NASA SnowEx campaign. The study site was a 1km<sup>2</sup> area located outside the Town of Moccasin, Judith Basin County, Montana at the MSU Central Agricultural Research Center (CARC) and represents a prairie biome with heavy agricultural activity. Data acquisitions, consisting of one “snow-off” and seven

“snow-on”, occurred between January 15<sup>th</sup> and March 4<sup>th</sup>, 2021. A 1550nm LiDAR system was used for the snow-off acquisition and a single snow-on sample acquisition to test the efficacy of 1550nm LiDAR for snow surface mapping. A 905nm LiDAR system was used for all snow-on acquisitions. A, a high accuracy adjusted control network, consisting of three substantial monuments, was established on site to tie the LiDAR acquisitions to a global coordinate system. Truthing and quality control points, referenced to this control network, were collected for each acquisition using GNSS survey equipment. Georeferenced and classified point clouds and normalized intensity images were produced for each acquisition. Point cloud classifications yielded ground and model key classes in the snow-off and snow-on point clouds that were used to produce one snow-off DTM and seven snow-on DSMs. All point clouds achieved at least USGS LiDAR Base Specification QL1 and ASPRS Vertical Accuracy Class IV. The model keypoints vertical tolerance of 0.10m allows accurate contours as fine as 0.20m to be generated. All products were processed to meet specific geodetic datum requirements (detailed in Table 2).

## Included Files and Folders

Final deliverable files and folders submitted via the FTP site are detailed in the table below.

File/Folder Name	Description
DTM and DSMs <i>(folder)</i>	Contains folders of ESRI Grid format DTM for snow-off acquisition and DSMs for snow-on acquisitions.
Project Boundary <i>(folder)</i>	Contains files used to define the project area in shapefile format
Report Figure Images <i>(folder)</i>	Contains the original screenshots and photos used to create figures in this report
Tiled LiDAR <i>(folder)</i>	Contains folders of points clouds for each LiDAR acquisition day. Each day's folder contains a "Classified" folder with tiles of the full, classified point cloud and a "Filtered" folder with tiles of the model keypoints class only.
SnowEx 2021 Moccasin MT LiDAR Quality Stats.xlsx	Excel file containing GNSS points used to compute and verify point cloud vertical shifts to achieve cloud-to-cloud alignment and global accuracy. Each sheet also shows quality statistics. Each snow-on acquisition day has a "Alignment" sheet and a "Global" sheet except for 1/15, which only has a "Global" Sheet.

## Materials and Methods

### LiDAR Systems and UAV

DJ&A, P.C. acquired LiDAR data using two LiDAR Systems. The first, used for the snow-off acquisition and a single snow-on test acquisition, was a Phoenix LiDAR Systems Ranger LR. This system is based on a Riegl VUX-1 LR LiDAR sensor, which uses a 1550nm wavelength laser. Our particular Ranger LR system uses a Northrup Grumman LN200C Fiber Optic Gyroscope (FOG) IMU, Novatel OEM 617 GNSS receiver, and Novatel Pinwheel GNSS antenna.

The second LiDAR system was a Phoenix LiDAR Systems miniRanger. This system, used for the snow-on acquisitions, is based on a Riegl miniVUX-2 LiDAR sensor, which uses a 905nm wavelength laser. LiDAR systems using a laser wavelength near 900-1000nm are known to yield better pulse returns off snow and ice compared to other common LiDAR laser wavelengths, such as 1550nm and 532nm. The particular miniRanger system used had an Inertial Labs IMU-P IMU, Novatel OEM 7720 GNSS receiver, and Novatel Pinwheel GNSS antenna.

The UAV used was a customized Freefly Systems ALTA X. Custom payload mounting hardware was fabricated to attach each LiDAR system to the UAV. Insulation modifications were made to the UAV and LiDAR systems to minimize electronic issues due to cold temperatures.



**Figure 1.** Freefly Alta X UAV with Riegl miniVUX-2 LiDAR system used for snow-on acquisitions.

## Flight Planning and Data Acquisitions

The 1km<sup>2</sup> project area was provided in shapefile format by Dr. Eric Sproles at MSU. This shapefile was converted to a .kml, which was then loaded into the ALTA QGroundControl (QGC) flight planning and control software. ALTA QGC is Freefly's customized version of the open-source QGC software. The 1km<sup>2</sup> area was divided into automated waypoint mission zones; three for the snow-off and four for the snow-on acquisitions. Automated flight mission parameters were configured to ensure appropriate scan line and point-to-point spacing for the LiDAR. Flight lines were spaced to ensure a conservative overlap of 40% minimum between LiDAR swaths at a field of view (FOV) half-angle of 45 degrees. A conservative approach was warranted due to the relatively new process of LiDAR snow surface mapping. The additional overlap provided more processing flexibility. The flight area, zones, and lines can be seen in figures 2-4. Flight and LiDAR parameters for each acquisition can be found in Table 1. Google Earth .kml files of the project area and flight zones are included with these deliverables.



**Figure 2.** 1km<sup>2</sup> project area outside of Moccasin, Montana. UAV LiDAR flight zones and automated flight missions were built from these extents.

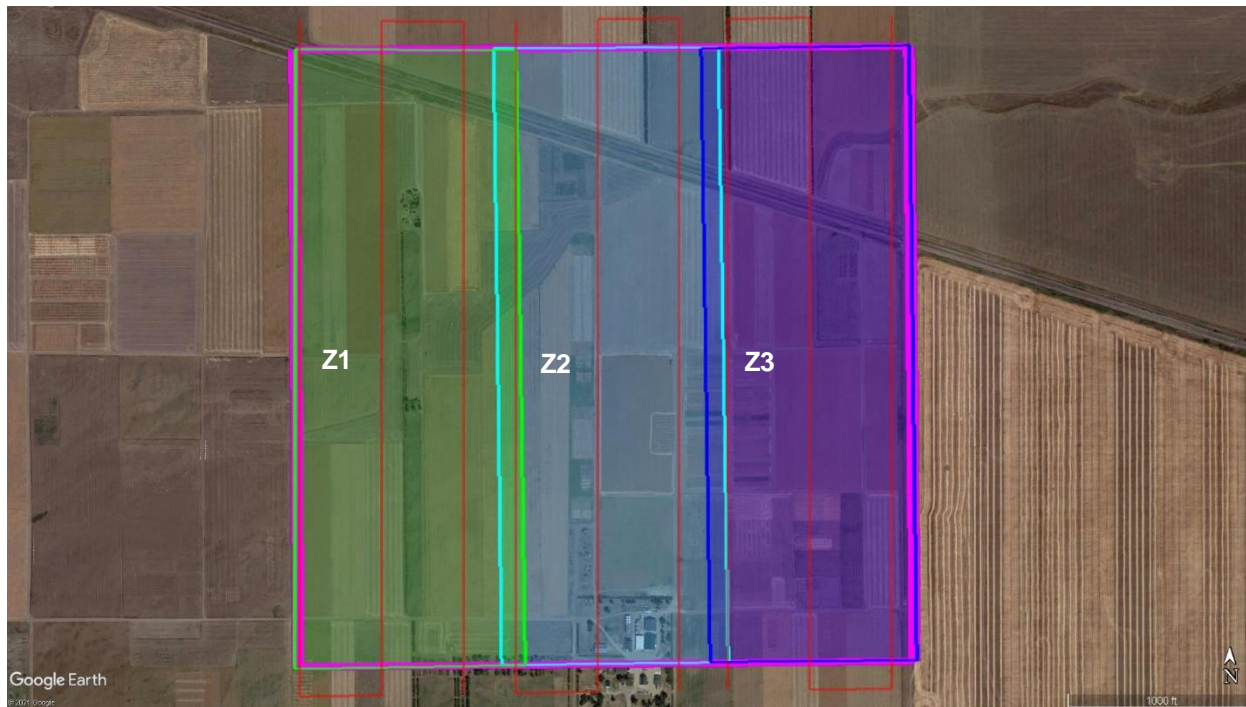


**Figure 3.** 1550nm snow-off flight zones and flight lines. Project area extents displayed in magenta. Three flight zones displayed in shades of green and blue. Flight lines displayed in red.

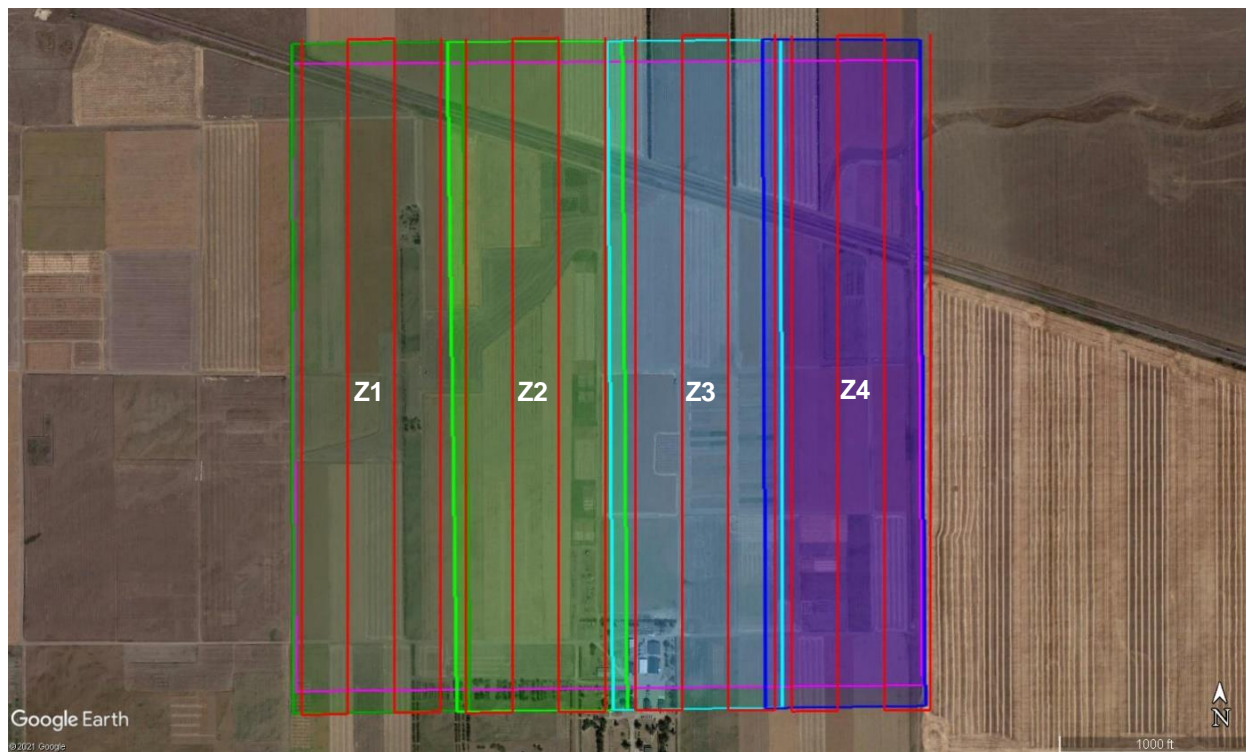


**Figure 4.** 905nm snow-on flight zones and flight lines. Study area extents displayed in magenta. Three flight zones displayed in shades of green and blue. Flight lines displayed in red. Note that the initial snow-on flight occurring on 1/21 used slightly different flight lines due to a 60m flight altitude. Subsequent snow-on flights used an 80m flight altitude and all their flight lines correspond to flight lines shown in this figure.

Date	Flight #	Flight Zone	Acquisition Type	Approx. Coverage	Laser Wavelength (nm)	Flight Alt. AGL (m)	Flight Speed (m/s)	Laser PRR (kHz)	Laser LPS	Temp. (°C)	RH	GPS Week
01/15/2021	1	1	Snow-off	100%	1550	120	6.0	820	200	-1	58%	2140
	2	2				120	6.0	820	200	-1	58%	2140
	3	3				120	6.0	820	200	-1	58%	2140
01/21/2021	4	4	Snow-on	100%	905	60	6.5	200	100	-5	66%	2141
	5	3				60	6.5	200	100	-5	66%	2141
	6	2				60	6.5	200	100	-2	47%	2141
	7	1				60	6.5	200	100	-2	47%	2141
01/22/2021	8	1	Snow-on	85%	905	80	7.0	200	100	-8	68%	2141
	9	2				80	7.0	200	100	-8	68%	2141
	10	3				80	7.0	200	100	-8	68%	2141
	11	4				80	7.0	200	100	-8	68%	2141
01/29/2021	12	1	Snow-on	100%	905	80	7.0	200	100	1	71%	2142
	13	2				80	7.0	200	100	1	71%	2142
	14	3				80	7.0	200	100	3	62%	2142
	15	4				80	7.0	200	100	3	62%	2142
01/29/2021	16	1	Snow-on (1550 test)	33%	1550	120	7.5	820	200	5	72%	2142
02/17/2021	17	4	Snow-on	100%	905	80	7.0	200	100	-9	92%	2145
	18	3				80	7.0	200	100	-9	92%	2145
	19	2				80	7.0	200	100	-9	92%	2145
	20	1				80	7.0	200	100	-9	92%	2145
02/18/2021	21	1	Snow-on	100%	905	80	7.0	200	100	-11	76%	2145
	22	2				80	7.0	200	100	-11	76%	2145
	23	3				80	7.0	200	100	-9	60%	2145
	24	4				80	7.0	200	100	-9	60%	2145
02/24/2021	25	4	Snow-on	85%	905	80	7.0	200	100	-4	70%	2146
	26	3				80	7.0	200	100	-4	70%	2146
	27	2				80	7.0	200	100	-4	70%	2146
	28	1				80	7.0	200	100	-4	70%	2146
03/04/2021	29	1	Snow-on	100%	905	80	7.0	200	100	4	46%	2147
	30	2				80	7.0	200	100	4	46%	2147
	31	3				80	7.0	200	100	4	46%	2147
	32	4				80	7.0	200	100	4	46%	2147

**Table 1.** All UAV LiDAR flights with respective flight and LiDAR acquisition parameters. Rows marked with red hashing indicate flights with issues that resulted in less than 100% data coverage of the study area. The zone 4 flight on 1/22 had to be abandoned due to strong winds. The zone 1 flight on 2/24 had an issue with the LiDAR system’s IMU mid-flight, which was not realized until office processing began. This resulted in a portion of that flight’s data being unusable.

AGL = Above Ground Level; PRR = Pulse Repetition Rate; LPS = Lines Per Second; RH = Relative Humidity

## LiDAR Truthing and Quality Control

The final LiDAR point clouds are intended to be compared to each other and used for snow volume calculations. To do this successfully, all point clouds must be horizontally and vertically aligned with each other with a high degree of accuracy. DJ&A employed two field methods to collect truthing and quality control data that was used to adjust and verify point cloud alignment. First, a minimum of 28 GNSS truthing points were collected for each acquisition using Trimble R10 GNSS base stations and rovers. Each truthing point was obtained via a 20 second/epoch minimum RTK shot. We attempted to achieve an evenly distributed random scattering of truthing points across the study area for each acquisition. However, access limitations due to mud and/or snow prevented an optimal distribution for all acquisitions. Regardless, we are confident that each set of truthing points was sufficient to allow a rigorous truthing process for their respective acquisitions. To collect truthing shots on the snow surface, we used a GNSS rover mounted on a survey rod and equipped with a laser distance meter to obtain accurate instrument height measurements for each shot. This provided a reliable and repeatable method for collecting snow surface truthing shots. The truthing equipment rigging is shown in figure 5. Laser measurements were periodically verified using a tape measure, which always showed agreement within 2mm.



**Figure 5.** A Trimble R10 GNSS receiver mounted on a survey rod equipped with a laser distance meter. By placing a reflective card on the snow surface, an accurate instrument height measurement to the snow surface could be obtained.



In addition to the truthing points, six triangular plates mounted on tripods were placed around the study area for each acquisition. The Northern vertex of each target was occupied twice with an RTK GNSS rover to obtain coordinates, which served as a quality control (QC) point. The first occupation was two minutes and the second, occurring after an RTK reinitialization, was one minute. Final coordinates for these targets were an average of the two occupations. These QC targets were captured in the LiDAR point clouds. By comparing each target's LiDAR points to its RTK GNSS shot, we were able to verify not only vertical, but also horizontal and rotational accuracy of the point clouds. The 3D truthing target construction and visualization in the point cloud is shown in figure 6. Raw truthing and QC point data can be found in the "SnowEx Moccasin MT 2021 GNSS Data" spreadsheet included with these deliverables.

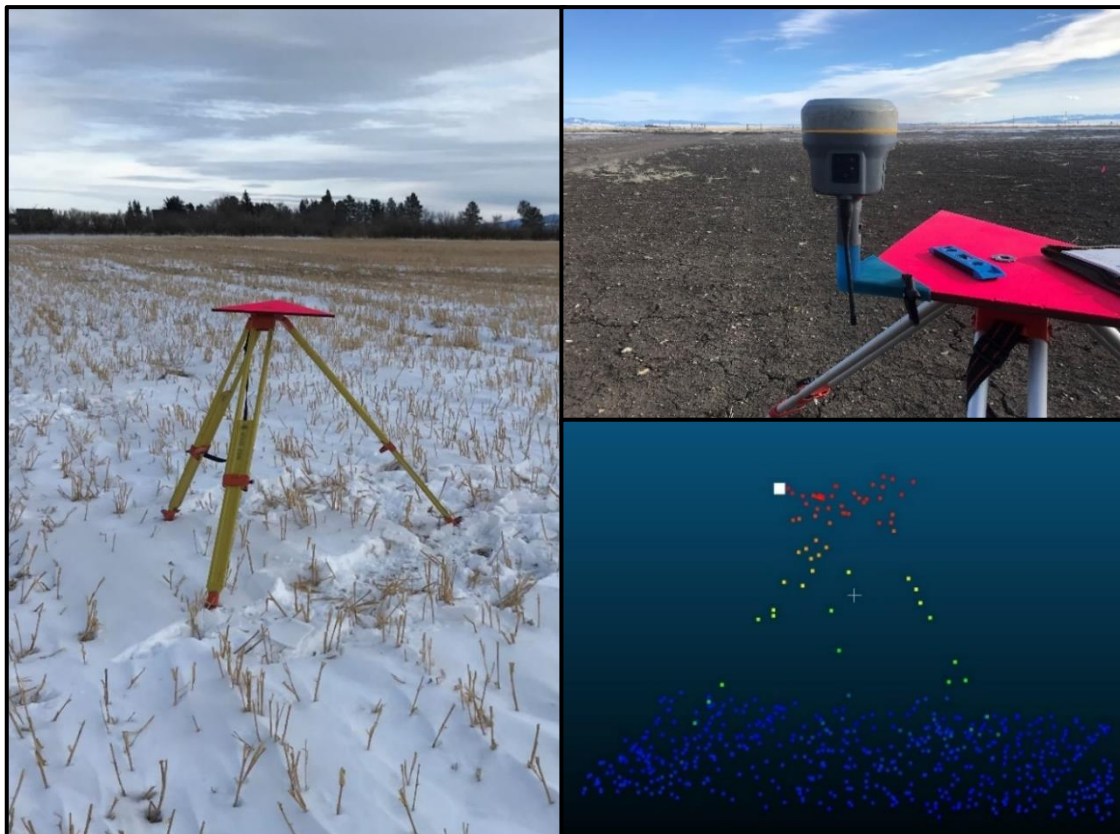


**Figure 6.** Six 3D control targets were placed around the study area for each acquisition. GNSS coordinates collected on the northern tip of these targets allowed for a quality control check on the point clouds' vertical, horizontal, and rotational accuracy. In the point cloud view, the target and ground are shown colorized by height. The GNSS point is colored white.

The 1/15 snow-off acquisition actually contained some snow cover along windbreaks. To obtain an accurate snow-off surface, we collected GNSS RTK shots along the edges of the major snowbanks/patches. 2D polylines constructed from these shots were used to clip out the point cloud inside the boundaries. The snow-off cloud and associated DTM has no data inside these areas.

Given the flatness of the site, we believe this provides a reasonably accurate model of the true ground surface. Two versions of the snow-off point cloud are included with these deliverables, one with the snowbanks clipped out and another with the snowbanks left in.

### GNSS Processing

The control network consisted of control points (CP) 1, 2, 3, and 4, which are 2-inch aluminum caps set on 5/8in x 30in rebar. CP-1, 2, and 3 were set at the start of the project. CP-4 was added later to provide a control point in a more convenient location. Each control point was occupied a minimum of two times for at least two hours each time with a Trimble R10 GNSS base station logging static observations. Prior to adding CP-4, a minimally constrained least-squares adjustment was performed to adjust the network to the OPUS solutions for CP-1, 2, and 3. Once CP-4 was added, it's two OPUS solutions were added to verify its baseline solution. The least-squared adjusted network was verified by comparing final each control point's final coordinates to its OPUS solutions. The control network was processed in Trimble Business Center with the geospatial parameters detailed in Table 2. Final coordinates for each control point are also provide in Table 2. These coordinates and the geospatial parameters are also available in the "SnowEx Moccasin MT 2021 GNSS Data" spreadsheet included with these deliverables.

Parameter		Specification	
Horizontal Datum		NAD83 (2011) (EPOCH:2010.0000)	
Horizontal Projection		UTM Zone 12 North	
Vertical Datum		NAVD88	
Geoid Model		Geoid 12B	
Horizontal Units		Meters	
Vertical Units		Meters	
Control Points			
Point 1		Point 2	
Latitude	N47°03'19.1806950"	Latitude	N47°03'19.2062766"
Longitude	W109°56'46.8032450"	Longitude	W109°57'24.5005839"
Ellipsoid Height	1280.471	Ellipsoid Height	1284.854
Northing	5211851.184	Northing	5211841.320
Easting	580022.499	Easting	579227.219
Elevation	1293.360	Elevation	1297.731
Description	2-inch aluminum cap marked "DJ&A Control Point"	Description	2-inch aluminum cap marked "DJ&A Control Point"
Point 3		Point 4	
Latitude	N47°03'49.9203299"	Latitude	N47°03'26.0404035"
Longitude	W109°57'10.3550868"	Longitude	W109°57'03.2761840"
Ellipsoid Height	1278.973	Ellipsoid Height	1281.397
Northing	5212793.398	Northing	5212058.263
Easting	579512.949	Easting	579672.145
Elevation	1291.891	Elevation	1294.287
Description	2-inch aluminum cap marked "DJ&A Control Point"	Description	2-inch aluminum cap marked "DJ&A Control Point"

Table 2. Project geospatial parameters and control point coordinates.

Truthing and QC points were exported in .csv format. Following ASPRS standards, each set of truthing points was randomly split into two subsets of roughly 75/25 proportions. The 75% subset is used to obtain a uniform vertical shift value to apply to the point cloud. The 25% subset is reserved for global/absolute accuracy reporting on the final point cloud elevation. Deviations from this standard process will be discussed in the “Snow Surface DSM Classification” section. In addition to the standard truthing process, our six QC target points served as an additional quality check. For the 3/4 acquisition, five GNSS points were collected on ice surfaces with the intent of using them to evaluate the accuracy of the 905nm LiDAR returns on ice.

### **LiDAR Trajectory Processing**

Mobile (aerial, terrestrial, aquatic, etc.) LiDAR systems collect a combination of GNSS and IMU/INS (Inertial Measurement Unit/Inertial Navigation System) data used to reconstruct an accurate and precise path of the sensor through space. For each data collection run, the GNSS and IMU datasets are combined using PPK (Post Processing Kinematic) methods. Novatel Inertial Explorer is used to compute a fixed-bias carrier phase solution in both the forward and reverse chronological directions to resolve a final SBET (Smooth Best Estimate Trajectory) of the sensor’s movement—i.e. the sensor’s accurate and precise path through space. This routine in Inertial Explorer also provides an SMRMSG file containing accuracy data for the trajectory. The resulting high quality trajectories are critical to the process of creating accurate point cloud products from LiDAR data. For this project, trajectories were processed to meet geodetic datum requirements as detailed in Table 2.

Figures 7 through 26 show the quantity of GNSS satellites, PDOP, and separations between paths independently generated from the GNSS and IMU data collected during each data acquisition run. Some runs covered single flights while others covered multiple. Thus, the number of charts shown below does not directly correlate with the number of flights performed. Brief changes in satellite numbers and occasional spikes in PDOP are normal and expected. GNSS satellite quantities of 6 or more are considered acceptable. PDOP at or below 5.0 is considered acceptable.

Graphs showing the separation between the sensor’s GNSS and IMU paths are used to evaluate the quality of the final trajectories, which are created by combining both of these datasets. Linear separations are shown in X, Y, Z (displayed as East, North, Up). Angular separations are shown as heading, roll, and pitch. GNSS and INS determined positions should be in close agreement with each other for a final trajectory to be considered high quality. X, Y, Z separation magnitudes of 0.02m or less are considered acceptable. Heading, roll, pitch separation magnitudes of 2 arcminutes or less

are considered acceptable. Heading values outside of 2 arcminutes for portions of the data acquisition are normal and expected. Localized spikes in both X, Y, Z, and heading, roll, pitch—correlated with aerial sensor calibration maneuvers and aircraft turns—are expected. The magenta boxes indicate the LiDAR data acquisition period.

## SnowEx 2021 Moccasin MT UAV LiDAR Report

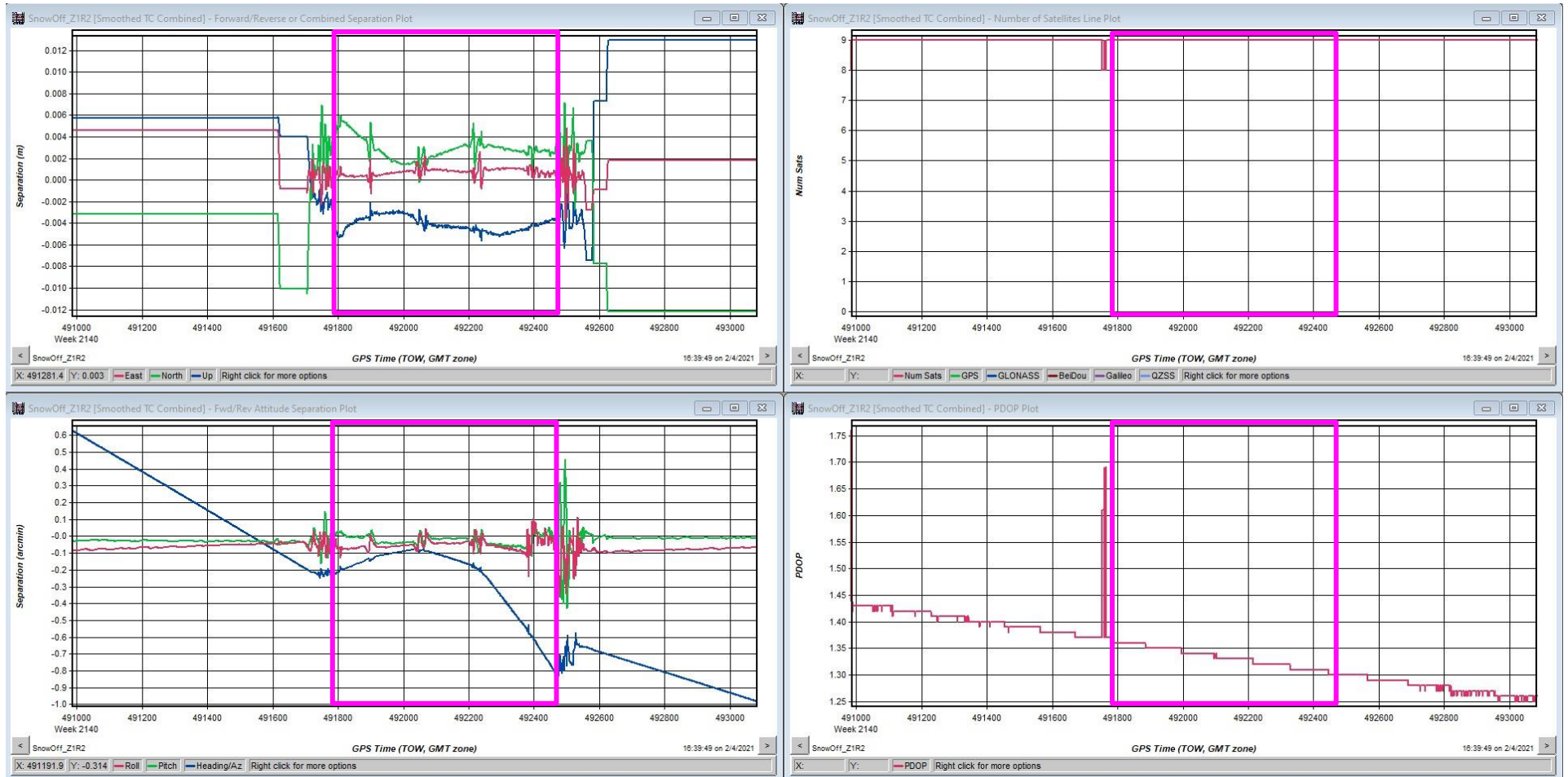


Figure 7. Snow-off 1/15 flight zone 1 PDOP, satellite quantity, and GNSS-IMU linear and angular separation plots.

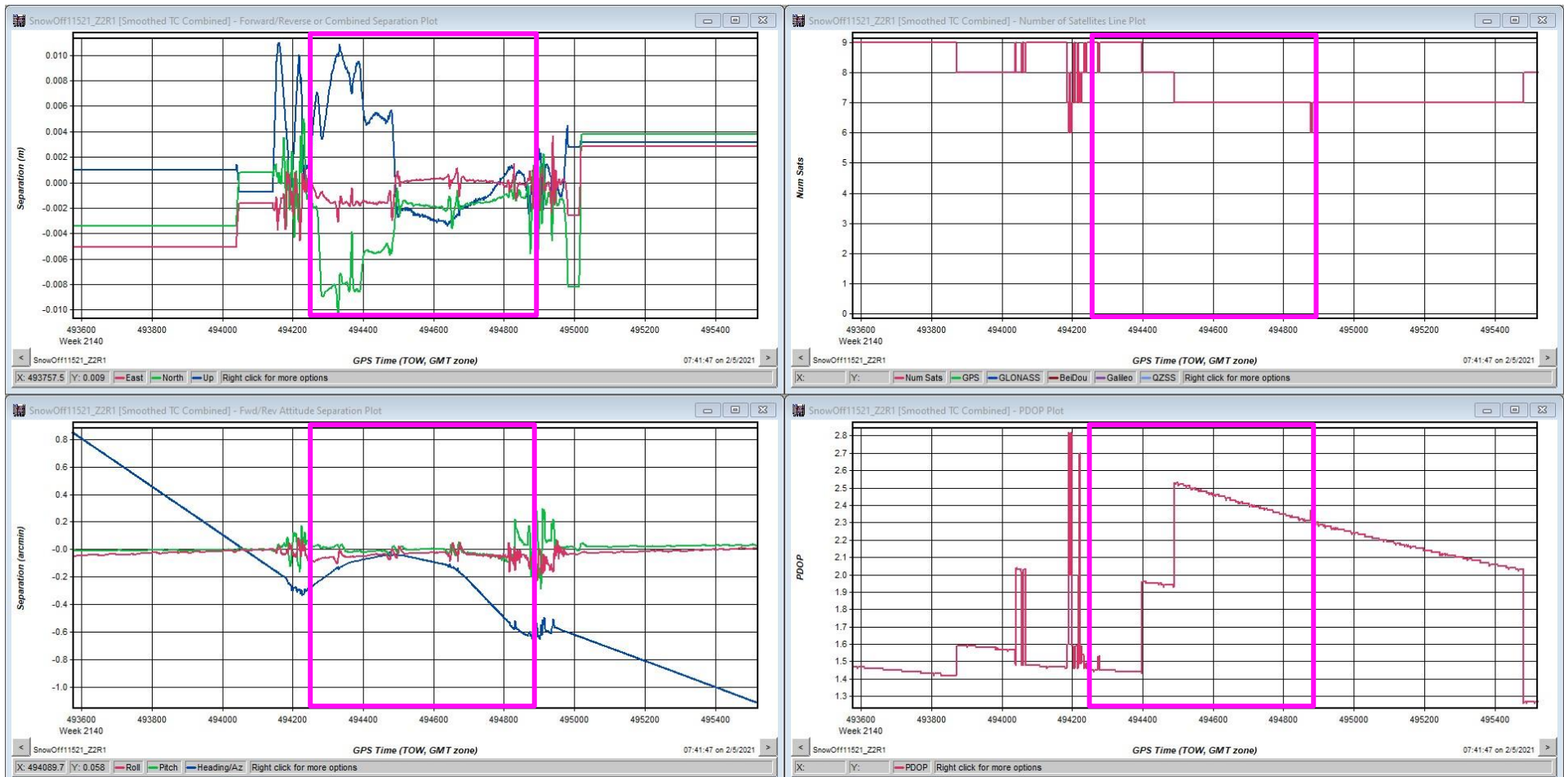


Figure 8. Snow-off 1/15 flight zone 2 PDOP, satellite quantity, and GNSS-IMU linear and angular separation plots.

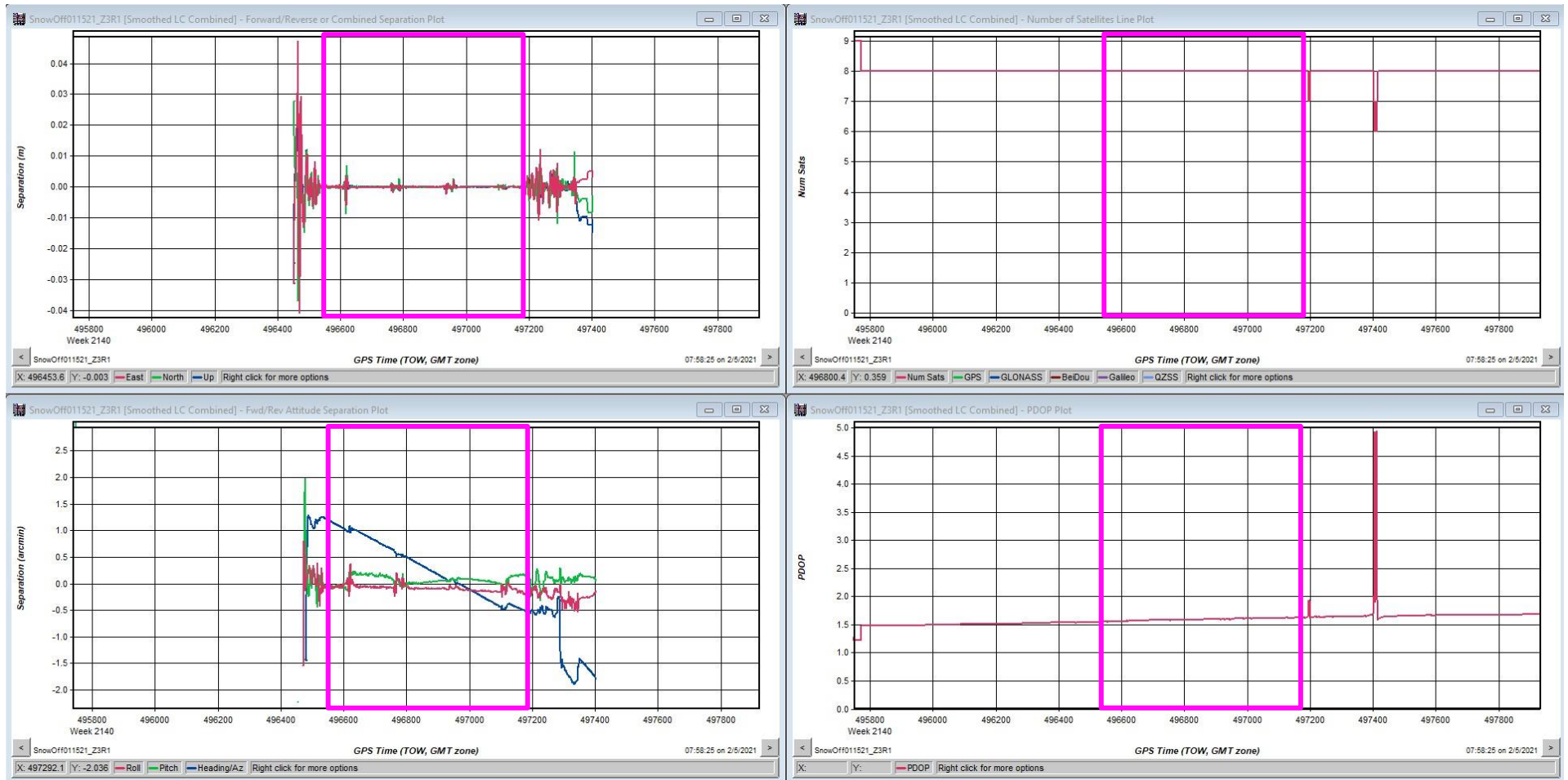


Figure 9. Snow-off 1/15 flight zone 3 PDOP, satellite quantity, and GNSS-IMU linear and angular separation plots.

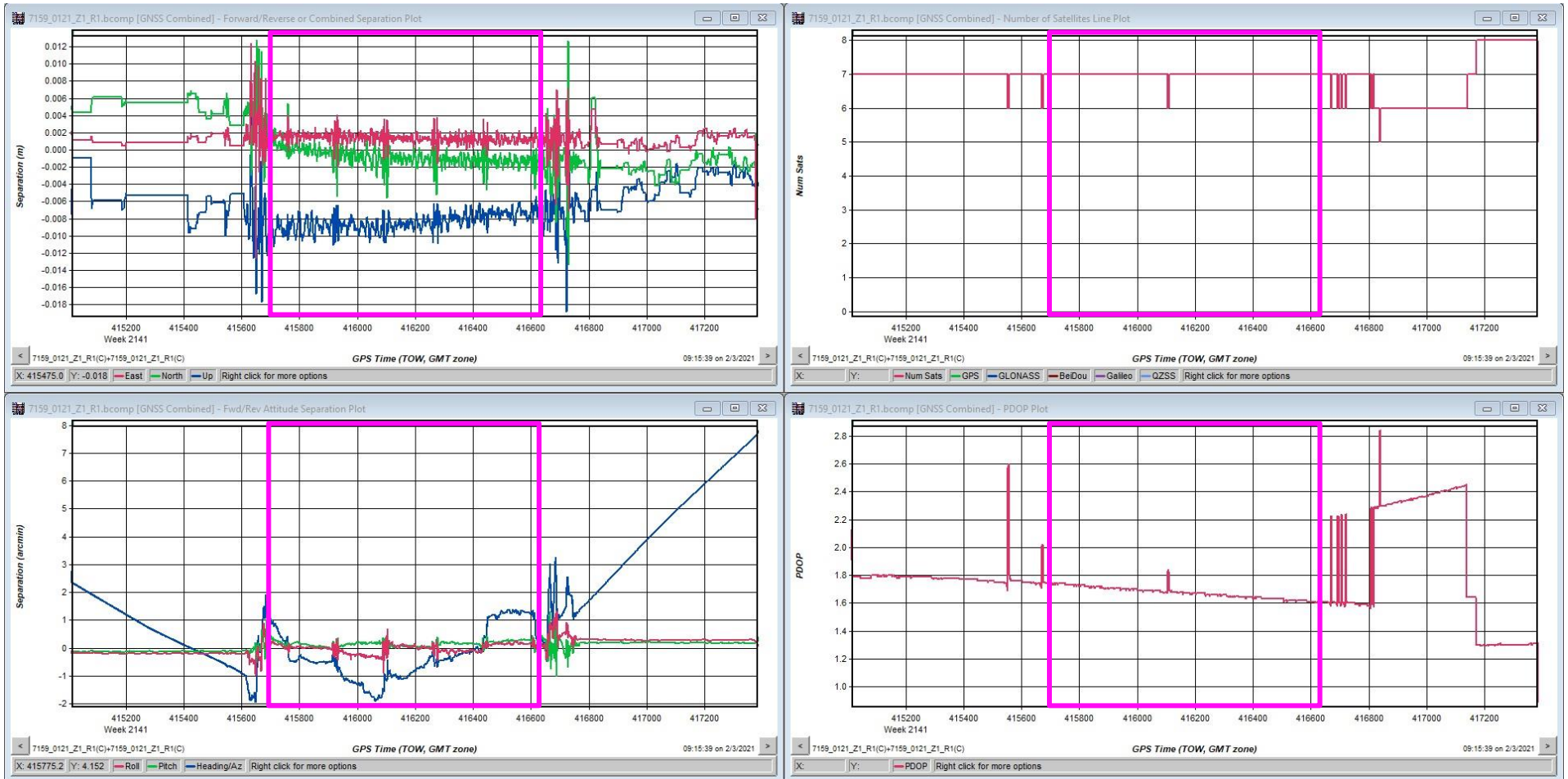


Figure 10. Snow-on 1/21 flight zone 1 PDOP, satellite quantity, and GNSS-IMU linear and angular separation plots.



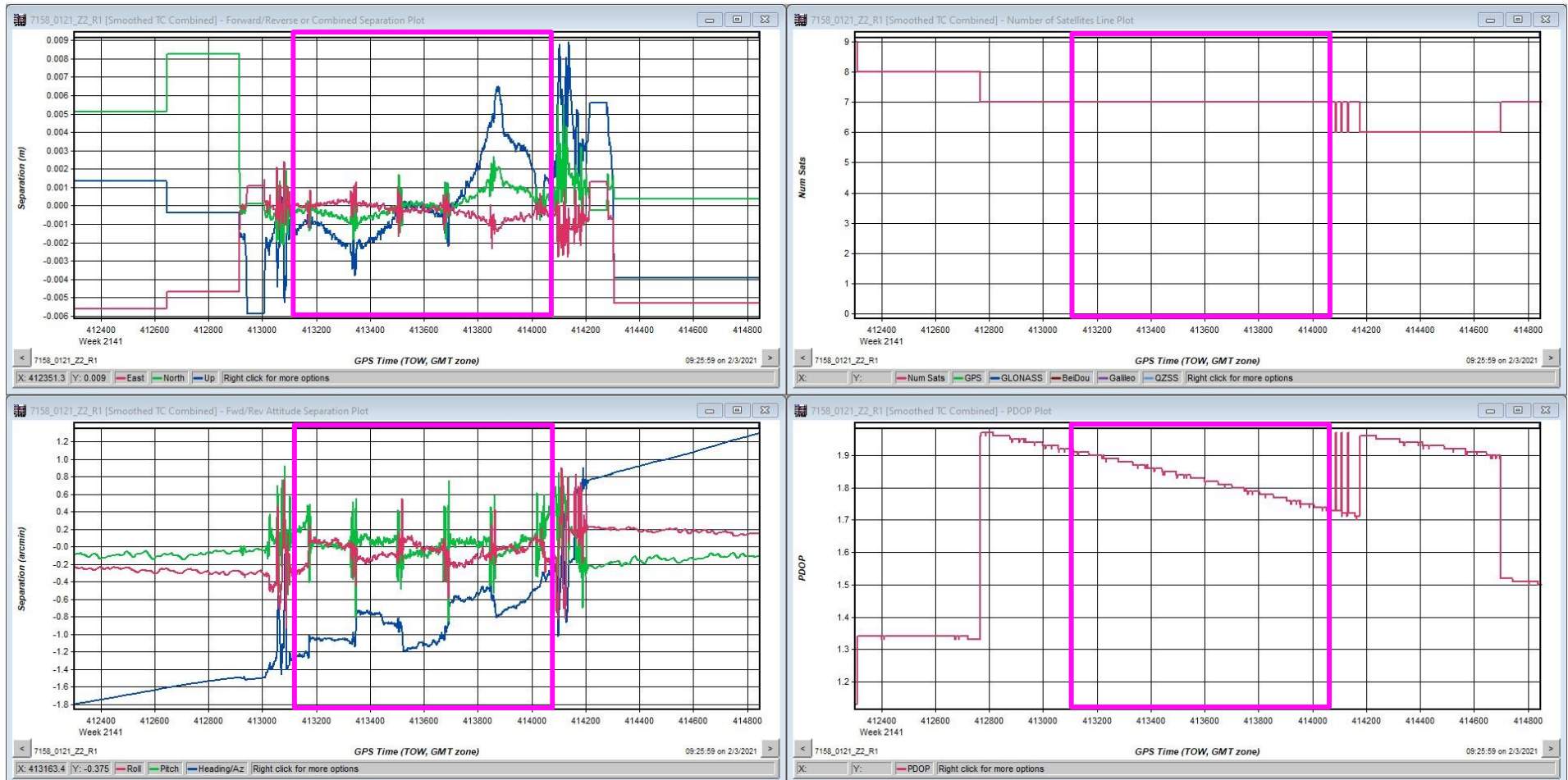


Figure 11. Snow-on 1/21 flight zone 2 PDOP, satellite quantity, and GNSS-IMU linear and angular separation plots.

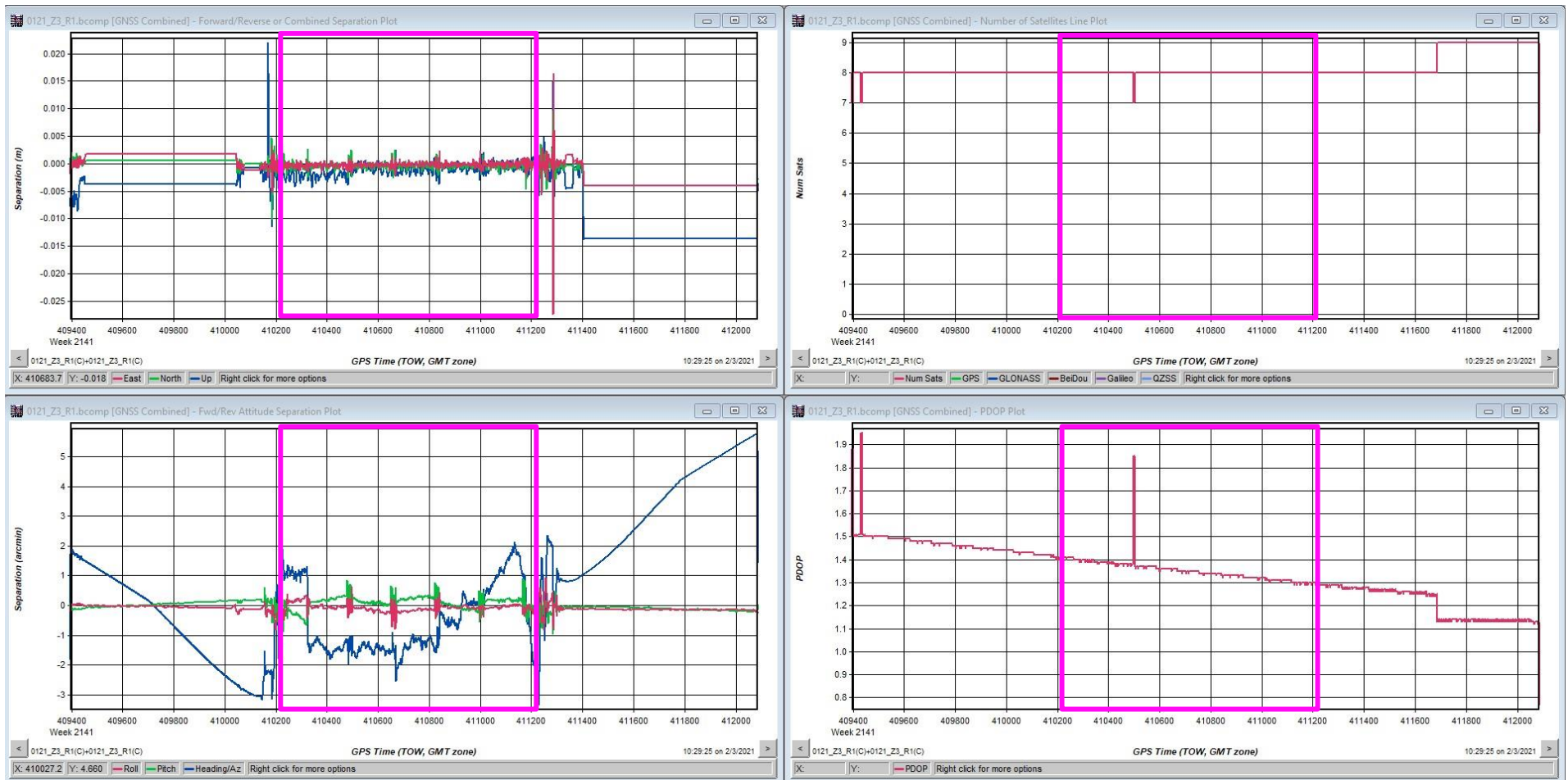


Figure 12. Snow-on 1/21 flight zone 3 PDOP, satellite quantity, and GNSS-IMU linear and angular separation plots.

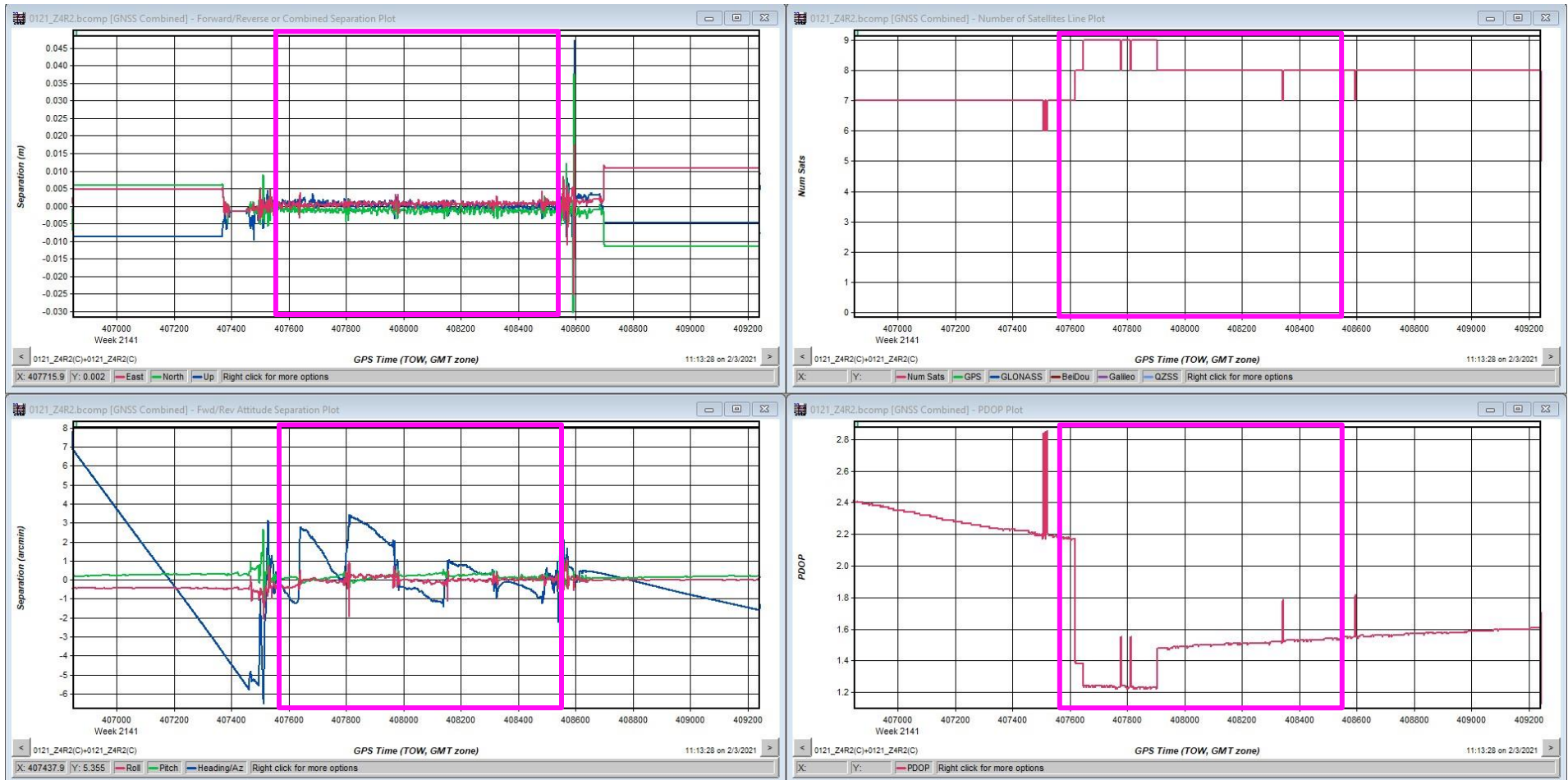


Figure 13. Snow-on 1/21 flight zone 4 PDOP, satellite quantity, and GNSS-IMU linear and angular separation plots.

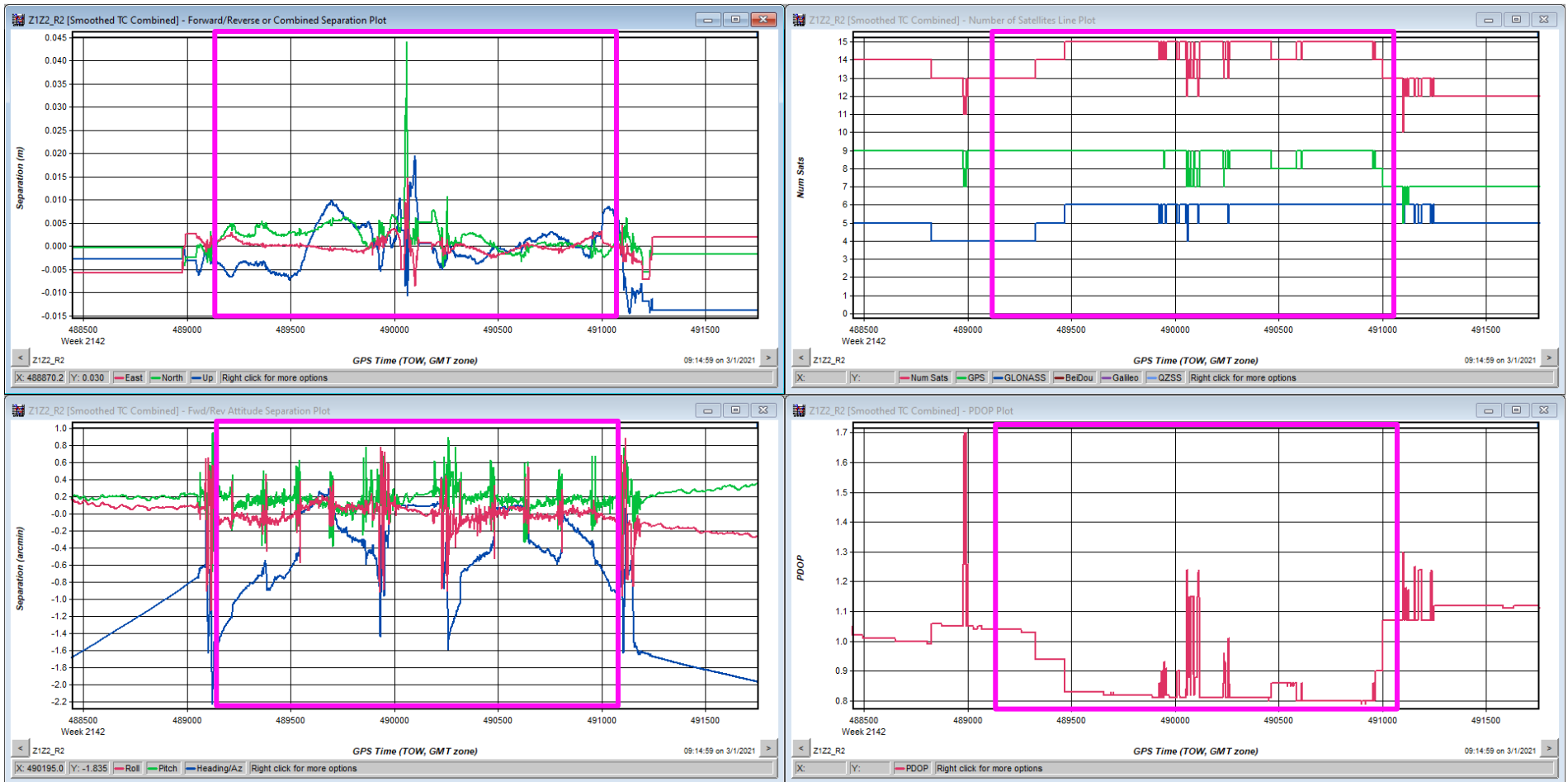


Figure 14. Snow-on 1/29 flight zones 1 and 2 PDOP, satellite quantity, and GNSS-IMU linear and angular separation plots.

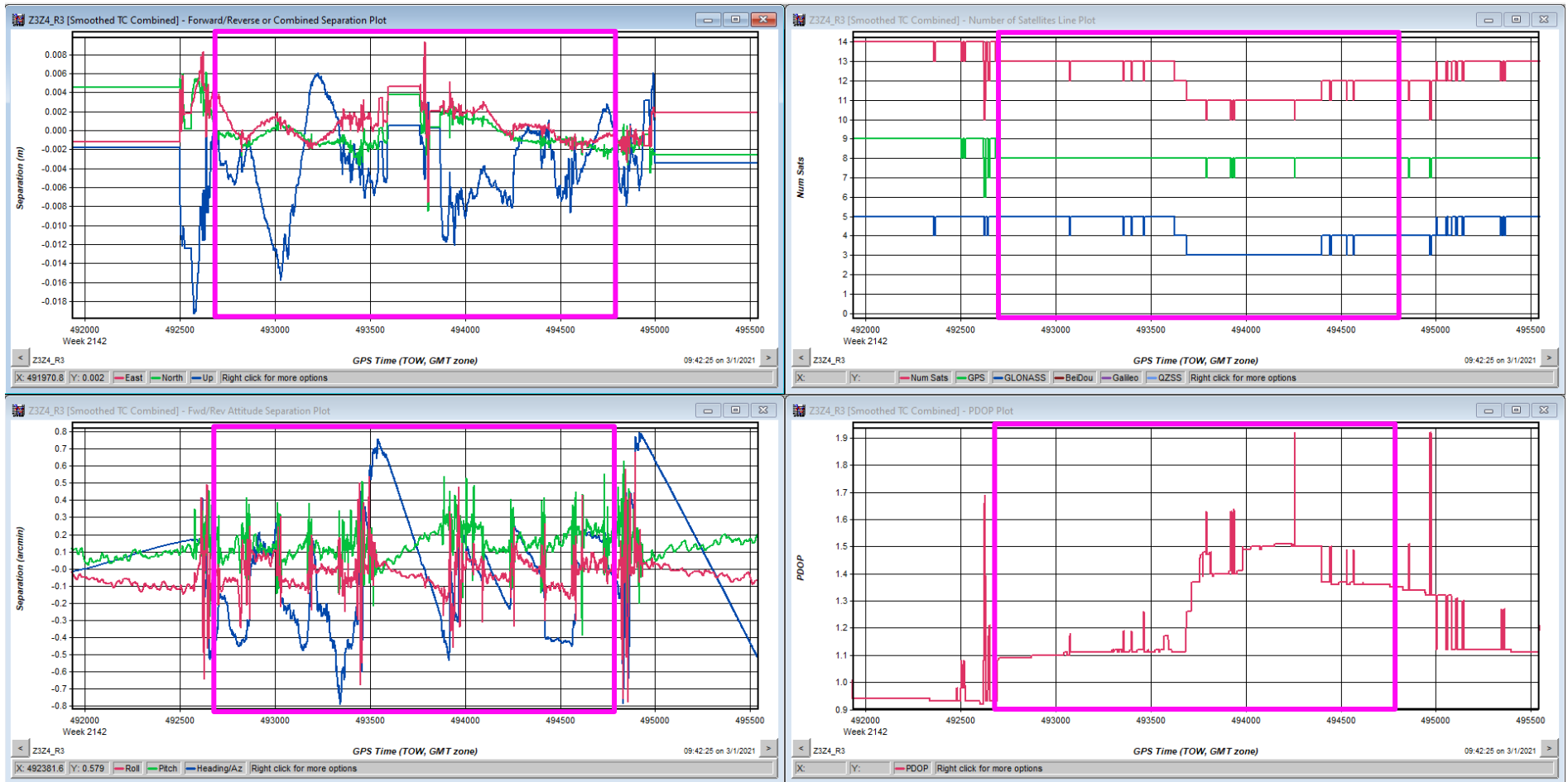


Figure 15. Snow-on 1/29 flight zones 3 and 4 PDOP, satellite quantity, and GNSS-IMU linear and angular separation plots.

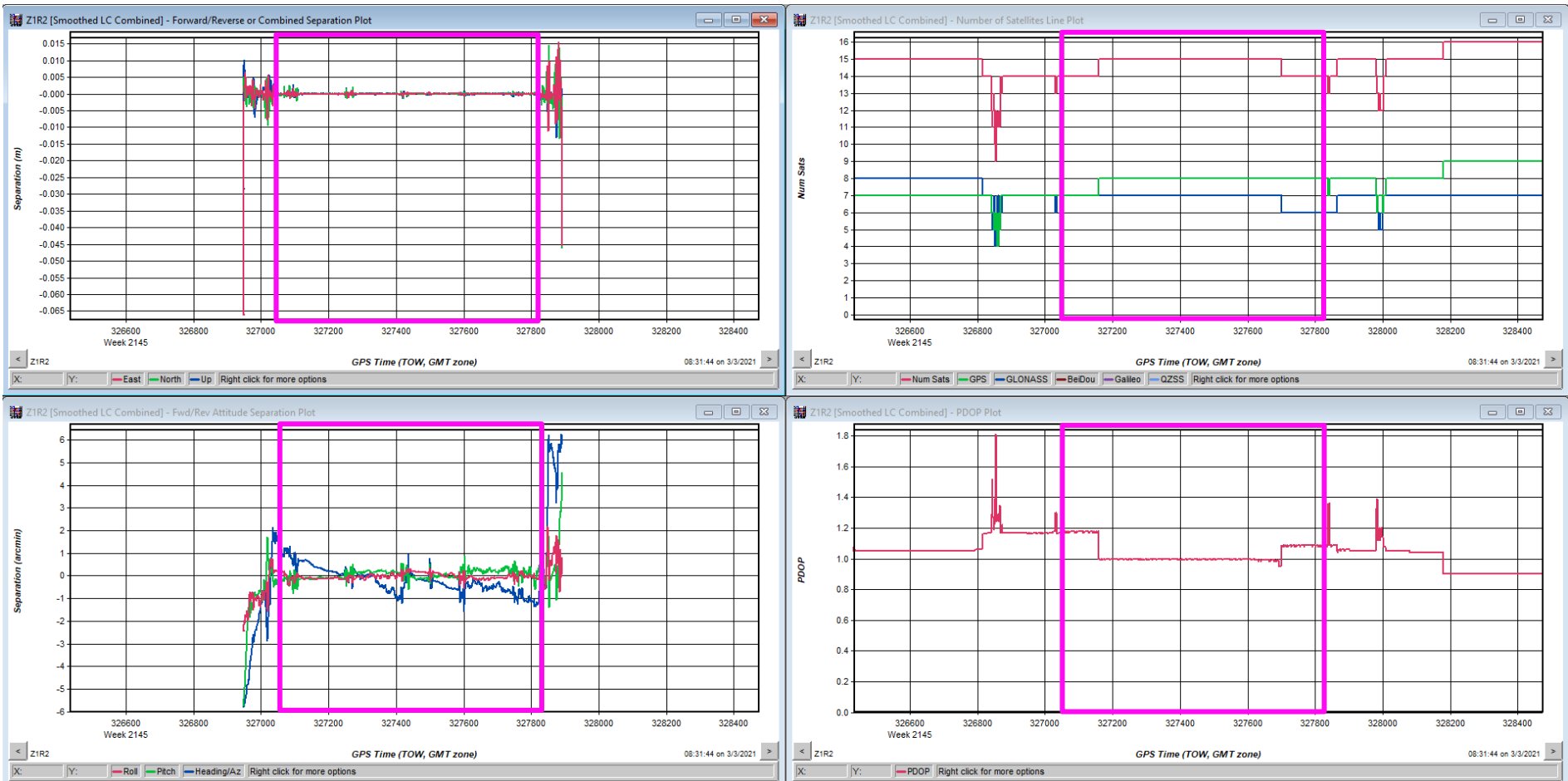


Figure 16. Snow-on 2/17 flight zone 1 PDOP, satellite quantity, and GNSS-IMU linear and angular separation plots.

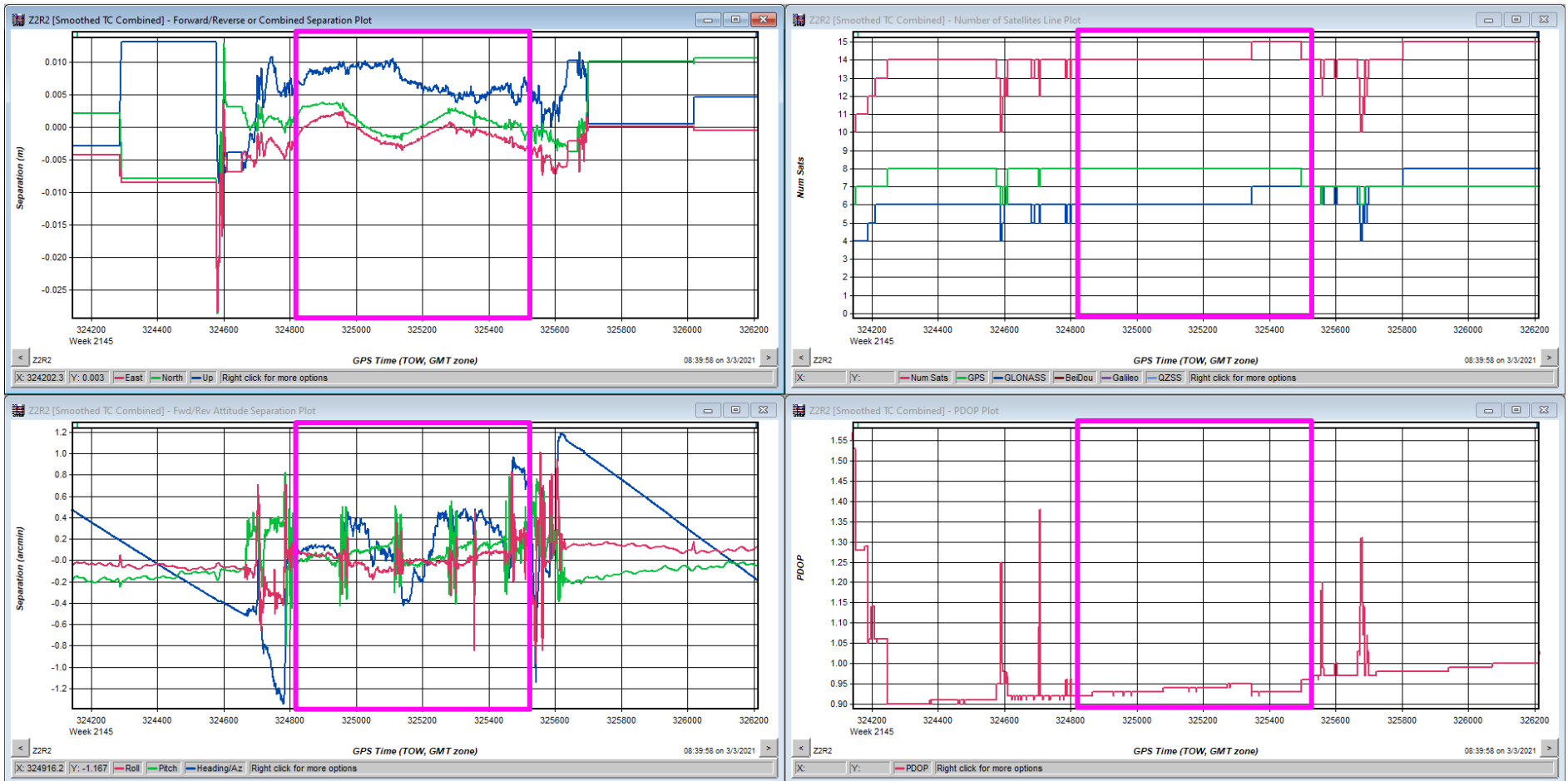


Figure 17. Snow-on 2/17 flight zone 2 PDOP, satellite quantity, and GNSS-IMU linear and angular separation plots.

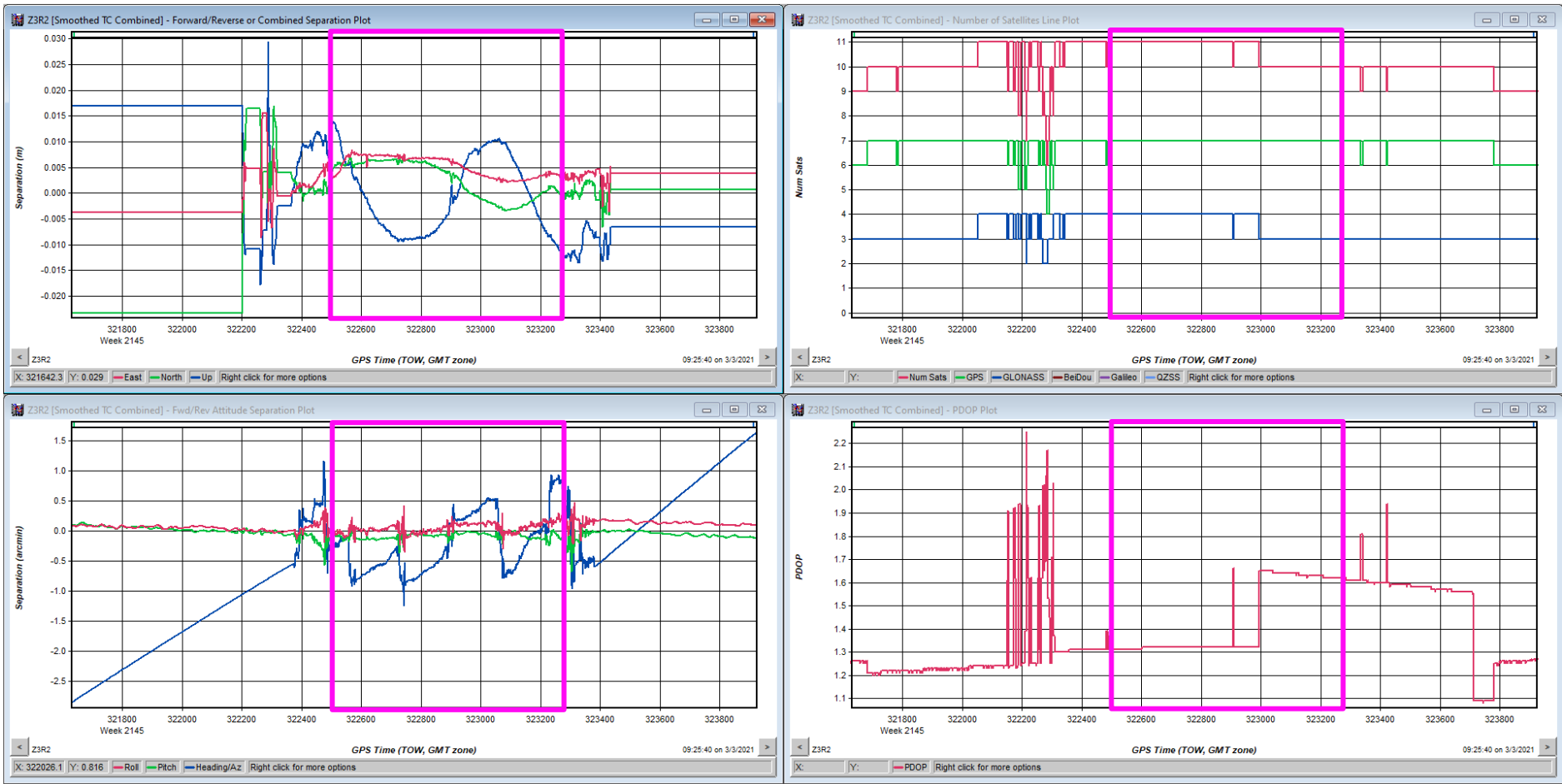


Figure 18. Snow-on 2/17 flight zone 3 PDOP, satellite quantity, and GNSS-IMU linear and angular separation plots.



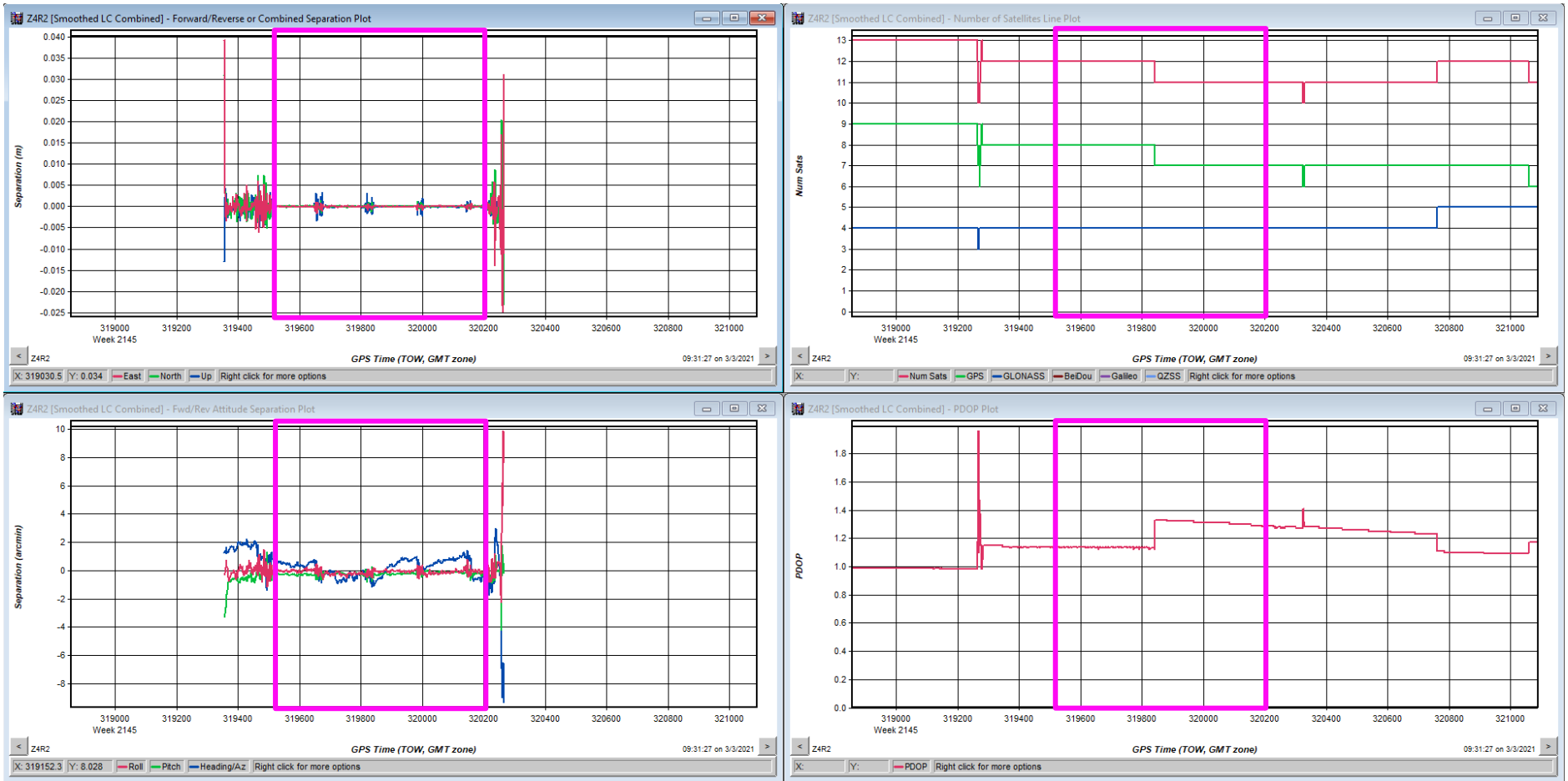


Figure 19. Snow-on 2/17 flight zone 4 PDOP, satellite quantity, and GNSS-IMU linear and angular separation plots.

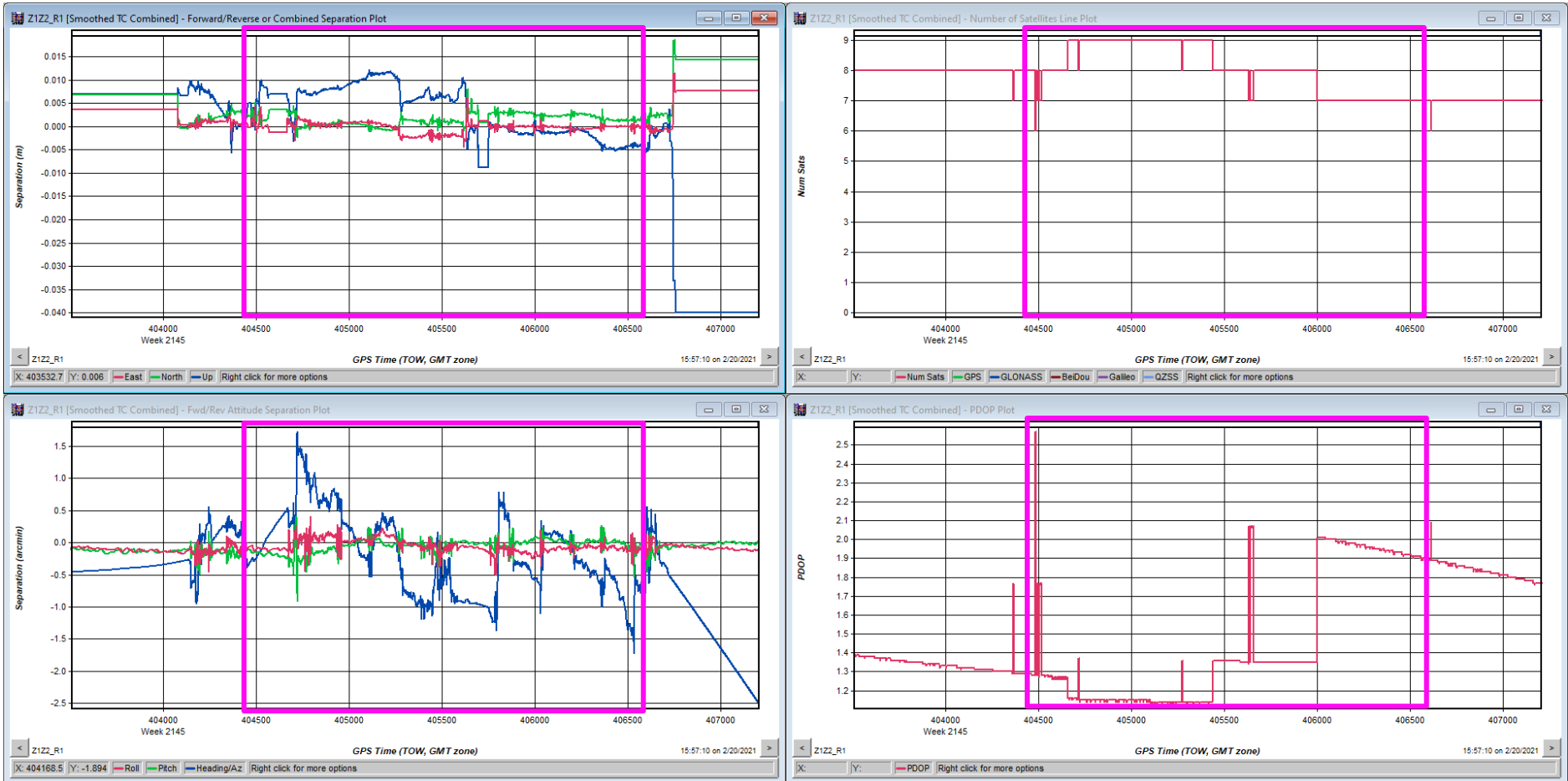


Figure 20. Snow-on 2/18 flight zones 1 and 2 PDOP, satellite quantity, and GNSS-IMU linear and angular separation plots.

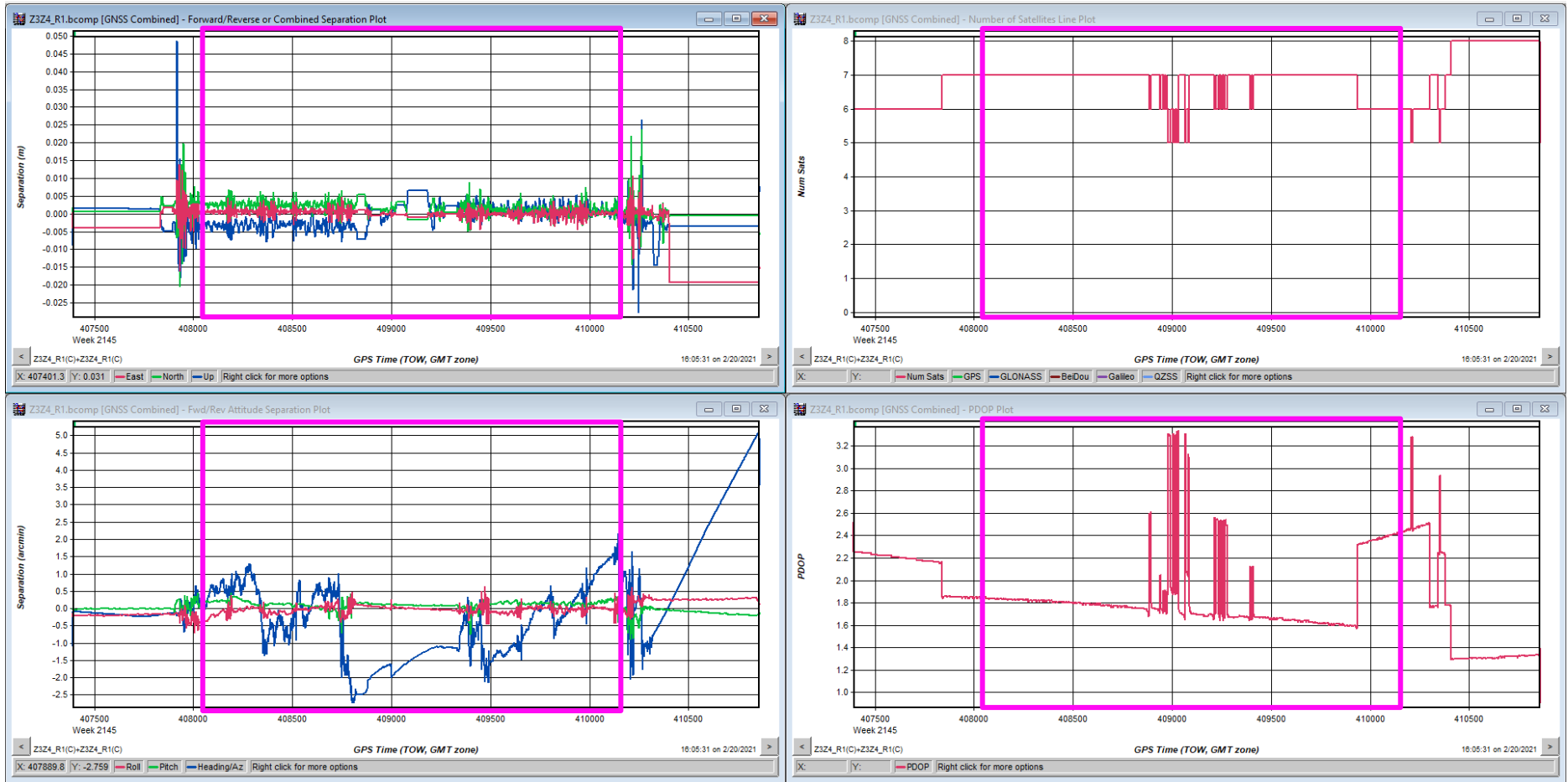


Figure 21. Snow-on 2/18 flight zones 3 and 4 PDOP, satellite quantity, and GNSS-IMU linear and angular separation plots.

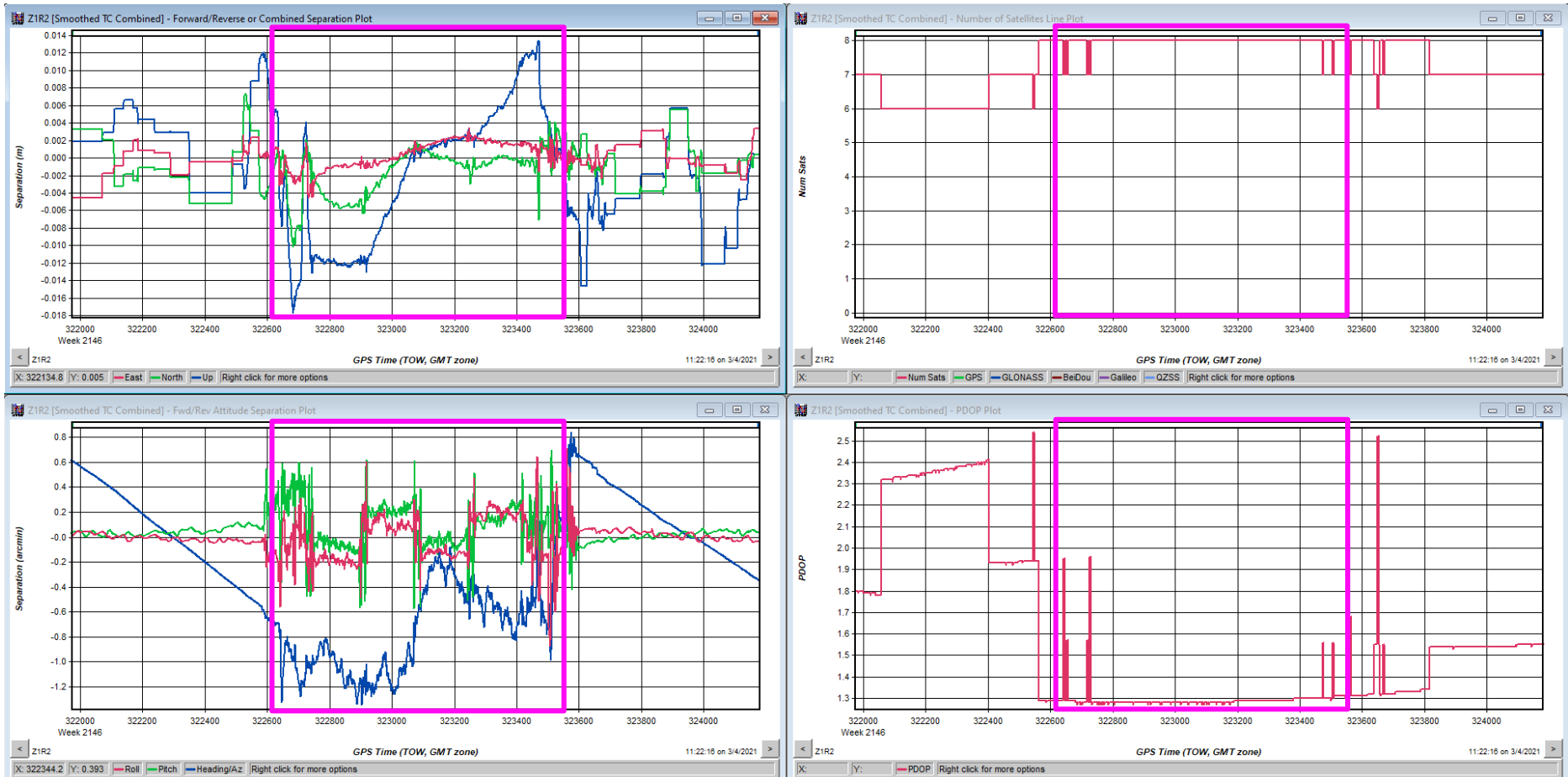


Figure 22. Snow-on 2/24 flight zone 1 PDOP, satellite quantity, and GNSS-IMU linear and angular separation plots.

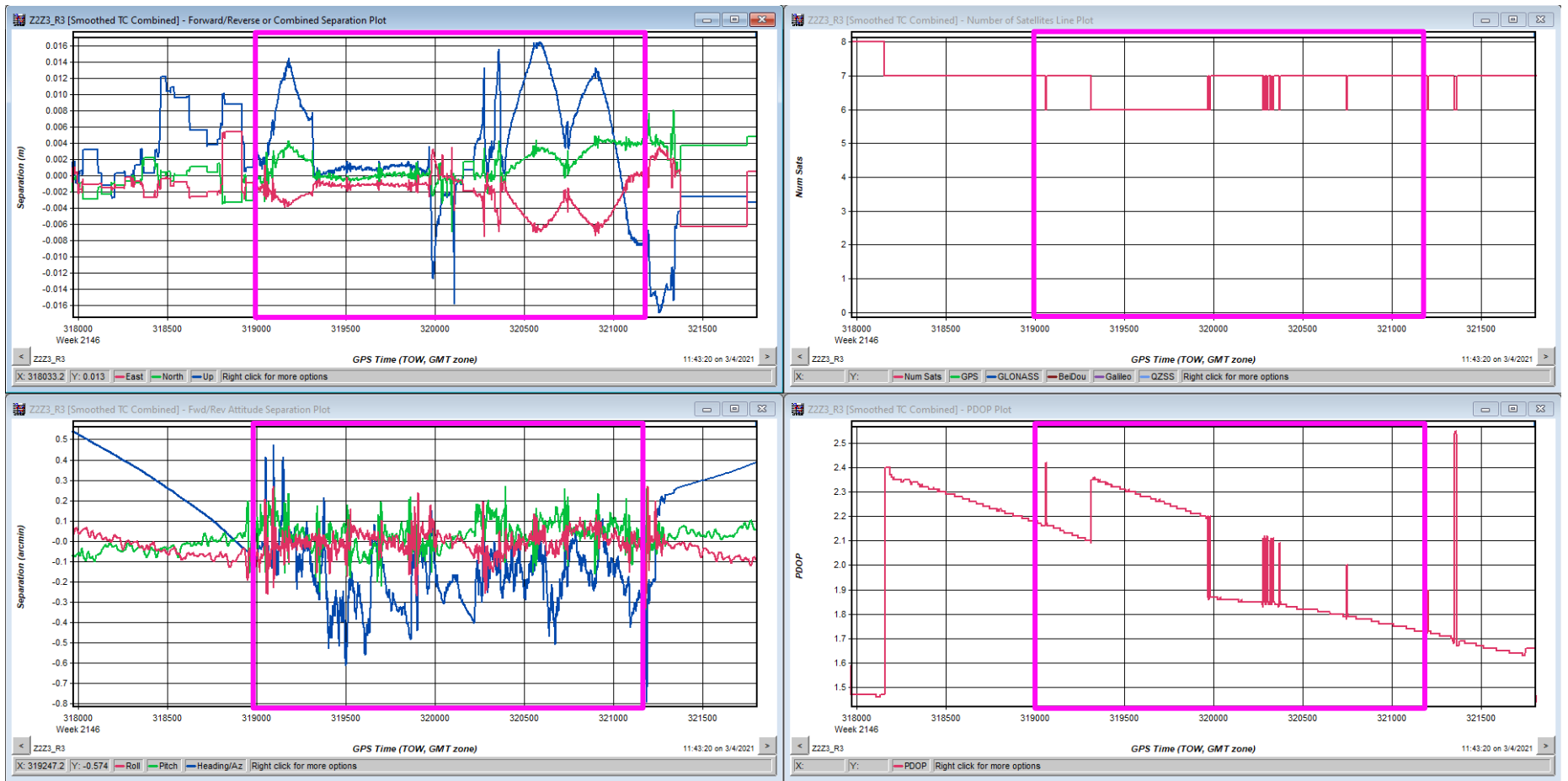


Figure 23. Snow-on 2/24 flight zones 2 and 3 PDOP, satellite quantity, and GNSS-IMU linear and angular separation plots.

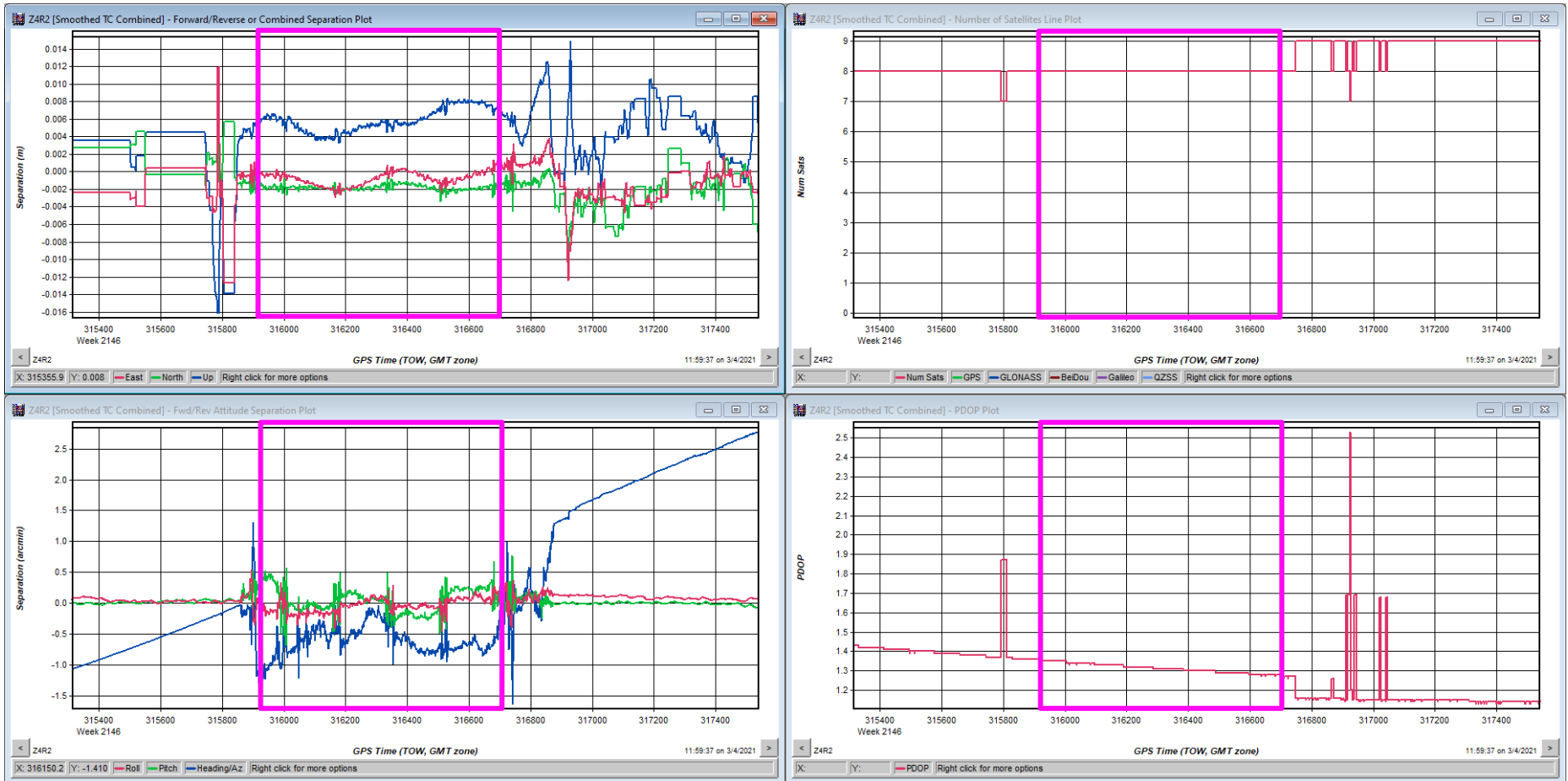


Figure 24. Snow-on 2/24 flight zone 4 PDOP, satellite quantity, and GNSS-IMU linear and angular separation plots.

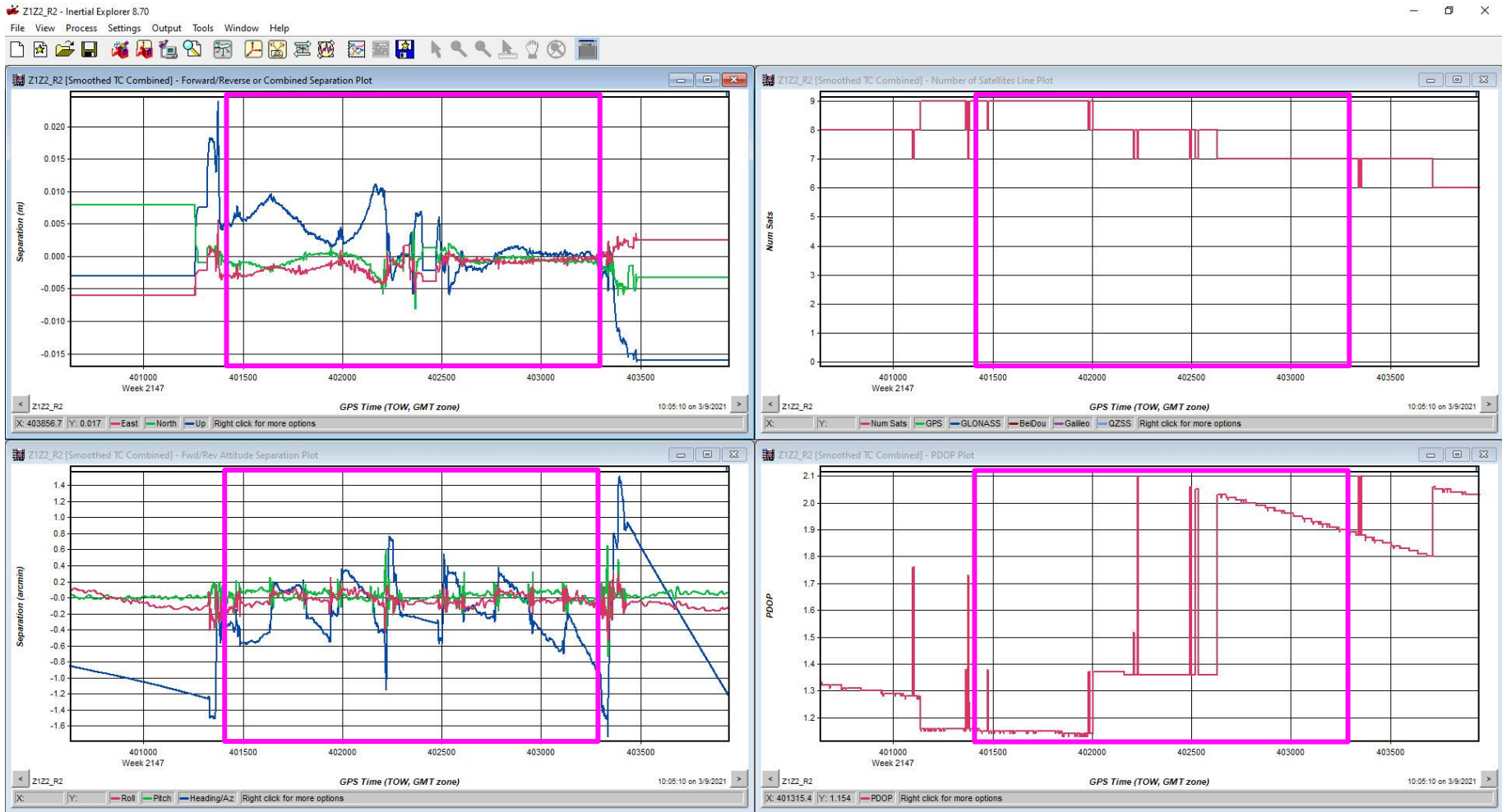


Figure 25. Snow-on 3/4 flight zones 1 and 2 PDOP, satellite quantity, and GNSS-IMU linear and angular separation plots.

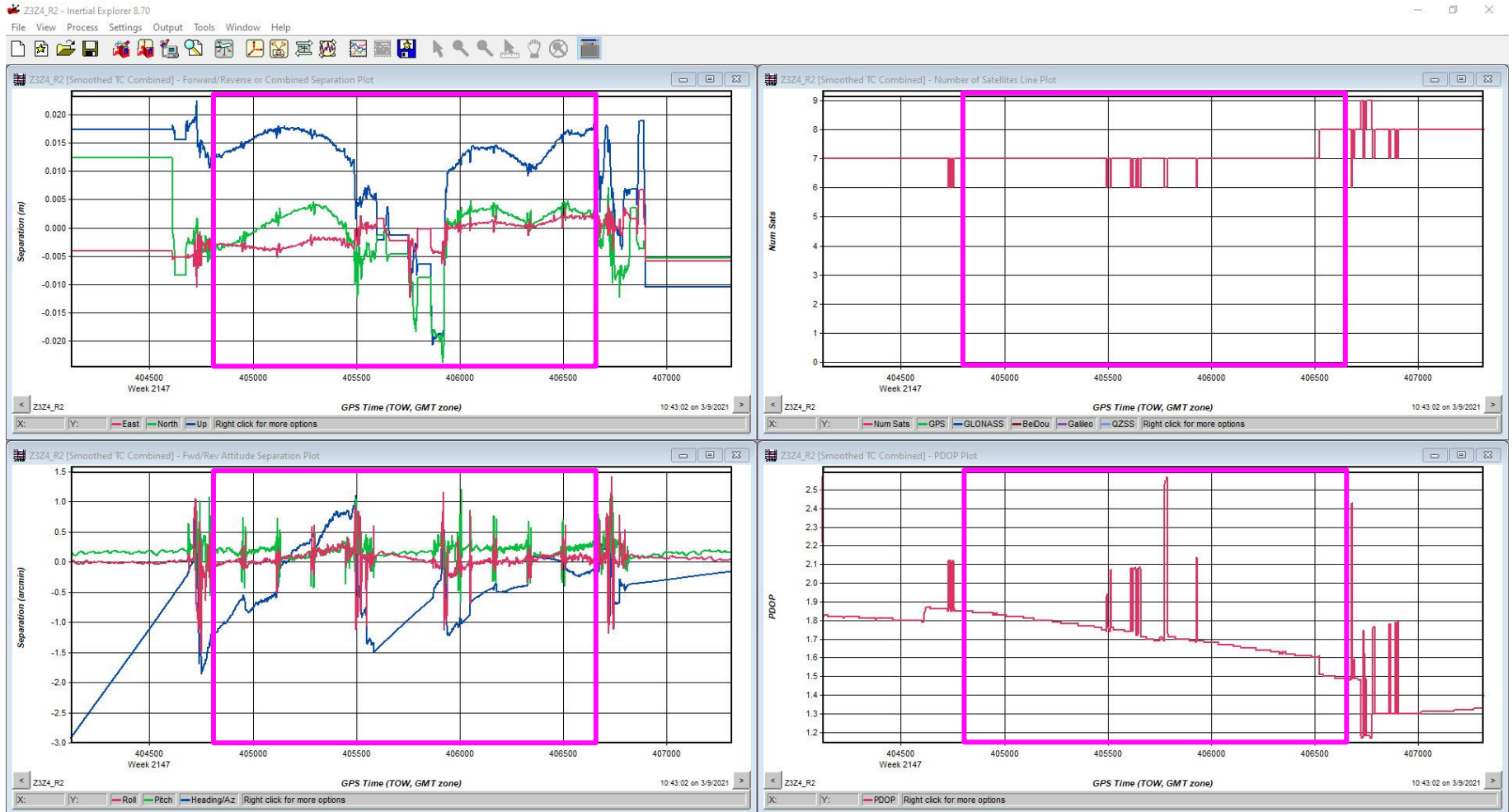


Figure 26. Snow-on 3/4 flight zones 3 and 4 PDOP, satellite quantity, and GNSS-IMU linear and angular separation plots.



## **LiDAR Point Cloud Generation and Typical Classification Methods**

With finalized trajectories, processing can proceed to the point cloud generation step. Riegl SDCImport was used to convert the raw LiDAR returns from Riegl's .rxp format to the .sdc format. The final trajectories, refined attitude data, and LiDAR returns in .sdc format were combined in Phoenix LiDAR Systems Spatial Explorer to generate point clouds in LAS format. The point clouds and finalized trajectories were imported into the TerraSolid mapping suite. The first step performed in TerraSolid is rectification between flight lines. Once a single unified cloud was obtained for each acquisition, we proceeded to manually clean noise out of the cloud, perform truthing procedures, and perform classifications to obtain a ground/surface and model keypoints classes for each cloud suitable for DTM/DSM generation. DSM classification of the snow-on surfaces required a unique approach. To understand the need for this approach, it is important to first understand the typical DTM ground classification process described below.

In any LiDAR point cloud, the true ground surface exists inside a layer of points near the ground. This "ground/surface thickness" occurs because of noise and inaccuracies introduced by a variety of factors including: surface characteristics, vegetation, imperfect flight line rectification, atmospheric conditions, and inherent inaccuracies of the LiDAR system components. For common natural surfaces (bare earth, vegetated fields, forest floors, etc.), this thickness is typically on the order of a few centimeters and the true ground surface exists somewhere near the middle of the thickness. Normally, we obtain a ground class using a single iteration of the TerraScan grounding algorithm. This algorithm searches for points along the bottom of the point cloud to include in the ground class—as opposed to the top which likely contains non-ground points like vegetation. This results in a ground class of points that represents the correct shape of the surface, but it is uniformly high or low relative to the true surface elevation. To adjust the point cloud to the correct elevation, we first generate a TIN surface from the ground class and run a comparison between it and the GNSS truthing points. This yields an average vertical offset ( $dz$ ) between the two. The GNSS points represent elevations of the true ground surface, so a "dz shift" is applied to the entire cloud to move it up or down towards the GNSS points. This results in a ground class with the correct shape located at the correct global/absolute elevation. Finally, model keypoints are extracted from the ground class and placed in their own class.

## **Snow Surface DSM Classification**

While attempting to classify a surface for the snow-on point clouds, it became apparent that the location of the true snow surface was not near the middle of the point cloud thickness, as is typical with other surfaces. Instead, our snow surface truthing points clearly showed that the actual snow surface is very close to the top of the point cloud. Additionally, all of the snow-on point clouds displayed larger than normal surface thickness and variation in thickness from day to day. Classifying the bottom of the point cloud and shifting it upwards to the truthing resulted in excellent alignment with its snow surface truthing points, but this caused the clouds to fall out of alignment with each other. This indicated that the bottom of the point cloud still represented an accurate surface shape, but the dz-shift—obtained in snow-covered areas—was not accurate for other parts of the point cloud such as vegetation, structures, and ground areas without snow (or even minimally snow-covered areas like plowed parking lots). Proceeding with the normal classification and shift process would result in unacceptable inaccuracies in these areas. In some cases, shifts of up to 15cm too high were observed. More importantly, the final DSM ground classes would not have been in good alignment with each other. If we had proceeded using the normal ground classification and shift methods, snow volume calculations based on the DTM and DSMs would have been less accurate than desired. A high precision of alignment between the point clouds is critical for accurate volume calculations.

To address this issue, we tried a “highest hit” DSM, which first requires vegetation and structures to be classified out and then the highest points of the remaining cloud to be classified as the surface. This yielded poor results. Even though care was taken to classify out as much vegetation as possible, it proved impossible to efficiently classify the majority of low vegetation. Vegetation classification algorithms work by choosing a starting height above which everything is classified as vegetation. To avoid mistakenly classifying actual surface points as vegetation, a large enough buffer value must be used to define the bottom of the vegetation class. Practically, a value of 0.15-0.30m is the smallest that can be used. This leaves behind the bottom parts of vegetation in the default class. When classifying a highest hit DSM, these pieces of vegetation would up in the surface class, which is undesirable. For normal topographic mapping, this is not usually an issue because the quantity of vegetation points left behind is insignificant. However, the large areas of crop residues protruding above the snow surfaces, combined with the high density of our point clouds, resulted in many vegetation points remaining in the DSM. Given the level of detail and accuracy we strove for on this project, we deemed this unacceptable and had to resort to a different method of DSM classification.

To ensure good alignment between point clouds while still maintaining an acceptable level of global accuracy, we developed custom ground classification and dz shift methods. Instead of running a

single instance of the ground classification algorithm, a custom macro was created to run five consecutive iterations. Each iteration placed its resulting points in a unique holding class, which effectively removed a layer of points from the bottom of the point cloud and cleared the way for the next grounding iteration to act higher up on the cloud. In this way, we were able to progressively move up through the point cloud towards the top. Five iterations were chosen to ensure the final one reached the top of the point cloud. In some cases, the fourth and fifth iterations went too far and began to include points from the bottom of vegetation and buildings. Another issue arose in areas where the point cloud thickness was thinner. In these areas the grounding iterations moved up through the cloud too quickly and eventually ran out of points to include in the later iterations. This resulted in areas with very few points included in the ground class. To avoid this issue, we manually reviewed the five iterations for each cloud and determined that, for all clouds, the third iteration was as close to the top of the cloud as possible without going too far. The third iteration was classified as the final surface and the four remaining iterations were classified back to the default class. The final ground class was also used to extract a model keypoints class.

### **Snow Surface Alignment and dz Shift**

After obtaining a ground/surface class for each cloud, we had to decide how to perform a vertical shift to align them with their truthing for global accuracy. In our first attempt, we tried the standard procedure of shifting each cloud by a unique value obtained from its truthing. This resulted in a very high degree of global accuracy for each cloud, but because each cloud's surface thickness was different, it once again caused them to become misaligned with each other. In particular, the snow-on clouds no longer aligned with the snow-off cloud in areas where they clearly should, such as buildings and other permanent structures. We decided that, for this particular application, alignment between clouds was more important than obtaining the best possible global accuracy for each cloud independently. By observing areas where all clouds should align (buildings, structures, cleared train tracks, snow-free/minimally snow-covered parking lots, etc.) we were able to determine that all clouds were in excellent alignment with each other prior to the dz shift. This indicated that all of the clouds should be shifted by approximately the same amount to keep them in alignment.

Instead of shifting each cloud by its own unique dz, we chose to obtain a dz shift value by comparing each snow-on cloud's model keypoints to the snow-off model keypoints in areas where they should align, such as cleared parking lots and train tracks. First, we extracted a subset of the snow-off cloud's model keypoints in these specific areas, then split them into approximate 75/25 subsets. The 75% subset was compared to a model keypoints TIN for each snow-on cloud to obtain a unique dz shift value, which was applied to its respective cloud. The remaining 25% was used to generate

statistics used to verify how well the shifted clouds aligned with the snow-off cloud. This approach allowed us to keep the clouds in good alignment with each other while still obtaining an acceptable degree of global accuracy. Additionally, for the snow-on clouds, we compared each cloud's keypoint TIN to its truthing points to obtain global accuracy statistics. Alignment and global accuracy statistics are presented in Tables 3-10 in the results section. These statistics and the points used to calculate them are also available in the "SnowEx Moccasin MT 2021 LiDAR Quality Stats" spreadsheet included with these deliverables.

### **Point Cloud Tiling and DTM/DSM Generation**

With the clouds aligned with each other and shifted for better global accuracy, we proceeded to generate two sets of tiles for each cloud using a 49 tile mesh. The deliverables include two folders of point cloud tiles for each acquisition. The "Classified" folder contains tiles of the entire point cloud classified into ground, model keypoints, and default. The "Filtered" folder contains tiles of only model keypoints. For the 1/15 snow-off acquisition, there are two additional Classified and Filtered folders appended with "\_NoSnowbanks". These tiles are identical to the regular Classified and Filtered tiles, but with the snowbanks discussed earlier clipped out. Finalized point clouds were exported in LAS 1.4 format. A shapefile of the tiling mesh and PDF map of the tiles are also included.

A snow-off DTM and snow-on DSMs were created in TerraScan using all ground points (ground and model keypoints classes). Cell size was set to 0.3m. The elevation value for each cell was computed as an average of the elevation values of all points in that cell. The DTM and DSMs were exported in ESRI Grid format.

### **Normalized Intensity Image Generation**

To perform normalization steps on the LiDAR intensity values, we used the TerraScan Scale Intensity macro. This tool applies a histogram matching adjustment to adjust the values of different intensity datasets to align with each other. We obtained median and spread values for each of the acquisitions using the View Histogram tool. Averages of these values were used to apply a scaling adjustment using the Scale Intensity macro's Stretch Spread method. This resulted in point clouds for each acquisition with intensity values adjusted to the same range. A raster was generated with 0.3m cell size. Each cell contains the average intensity of all points that fall within it. The final intensity images were exported as GeoTIFFs and tiled with the same tile mesh as the point clouds.

## Results

### Point Clouds

The final point clouds display a high degree of alignment with each other. This is evidenced through the alignment area model keypoints comparisons and visual inspection. Tables 3 through 10 contain the alignment statistics. Figures 27-33 show example qualitative evidence of point cloud alignment.

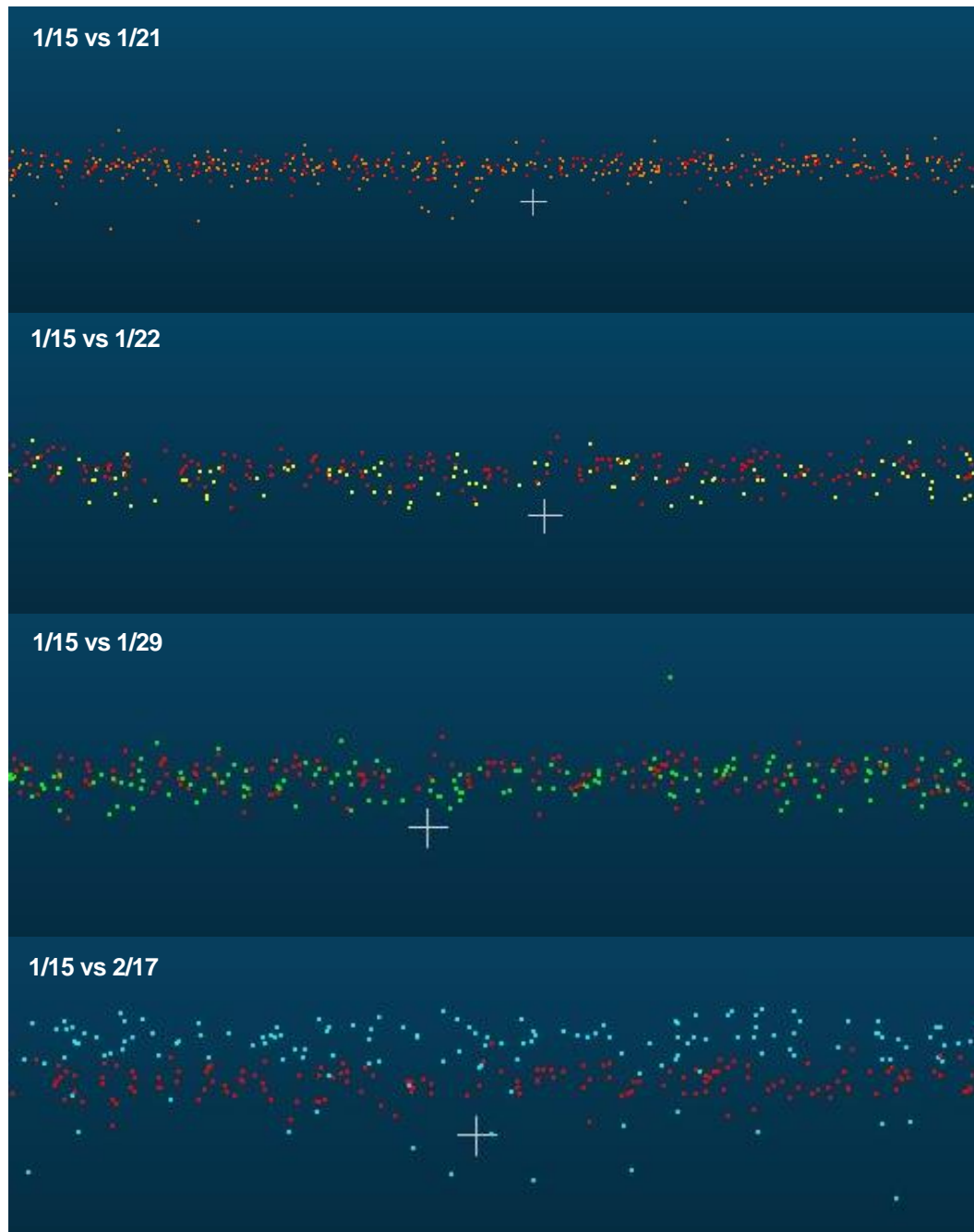


**Figure 27.** Profile detail of parking lot showing alignment between the 1/15 snow-off cloud (red) and the 1/21, 1/22, 1/29, and 2/17 snow-on clouds (orange, yellow, green, and cyan). Note the 2/17 cloud sits higher than the 1/15 cloud. This corresponds to field observations that the parking lot was not fully plowed on this day.

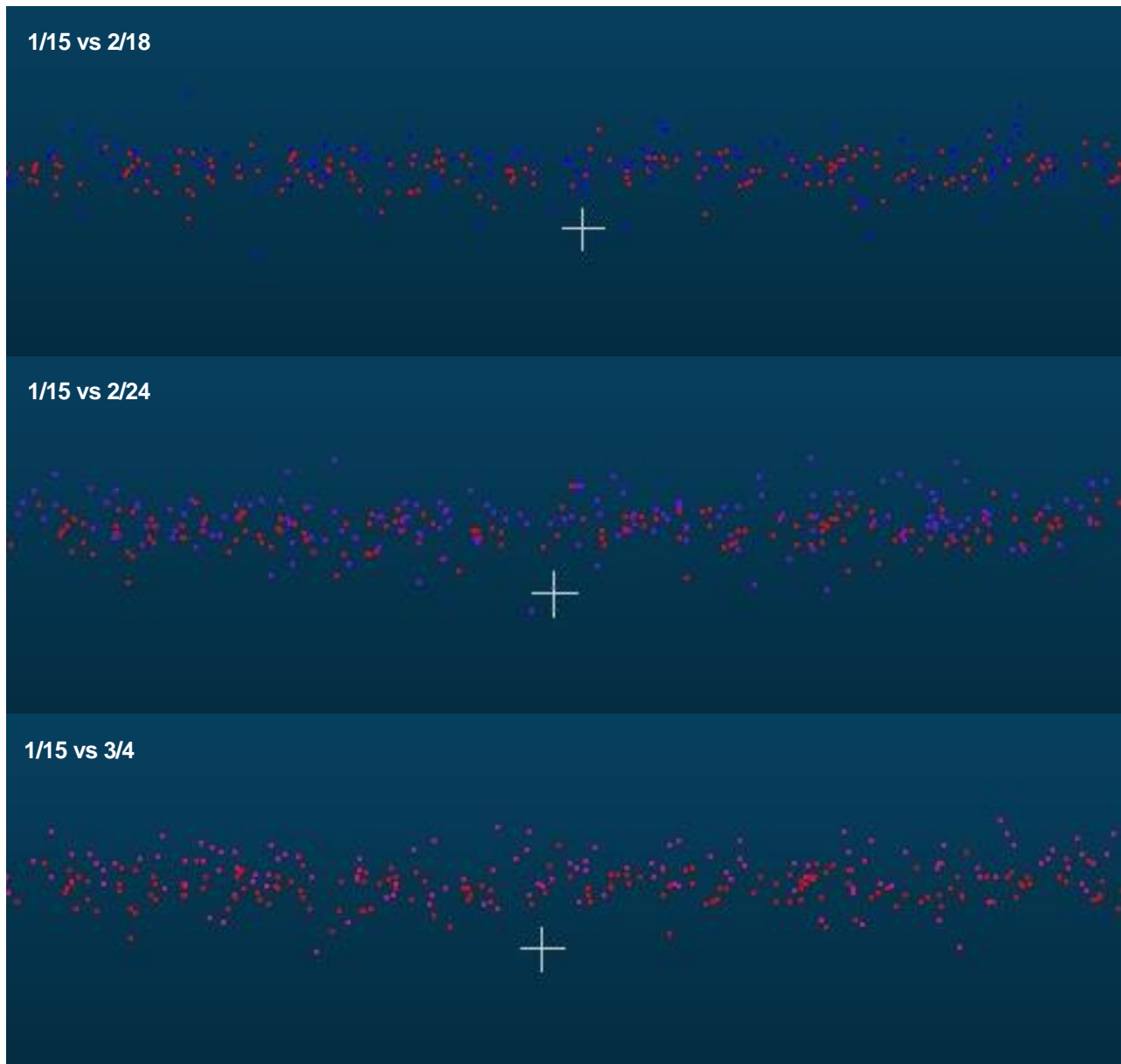


**Figure 28.** Profile detail of parking lot showing alignment between the 1/15 snow-off cloud (red) and the 2/18, 2/24, and 3/4 snow-on clouds (blue, violet, and magenta).

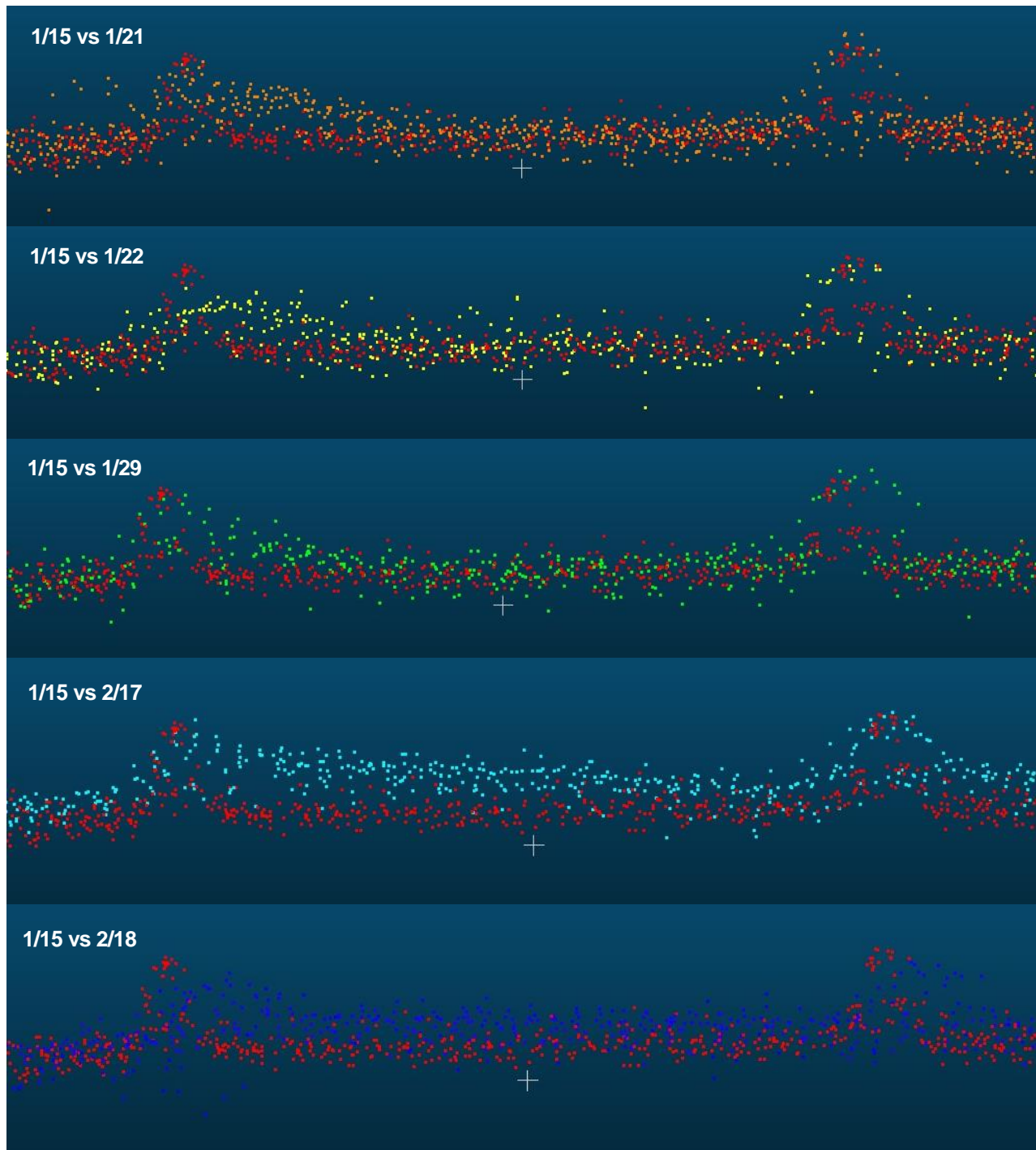


**Figure 29.** Profile detail of train tracks showing alignment between the 1/15 snow-off cloud (red) and the 1/21, 1/22, 1/29, 2/17, and 2/18 snow-on clouds (orange, yellow, green, cyan, and blue). Note the 2/17 and 2/18 clouds sit noticeably higher than the 1/15 cloud. This corresponds to field observations that snow was present on the railroad ties on these days.

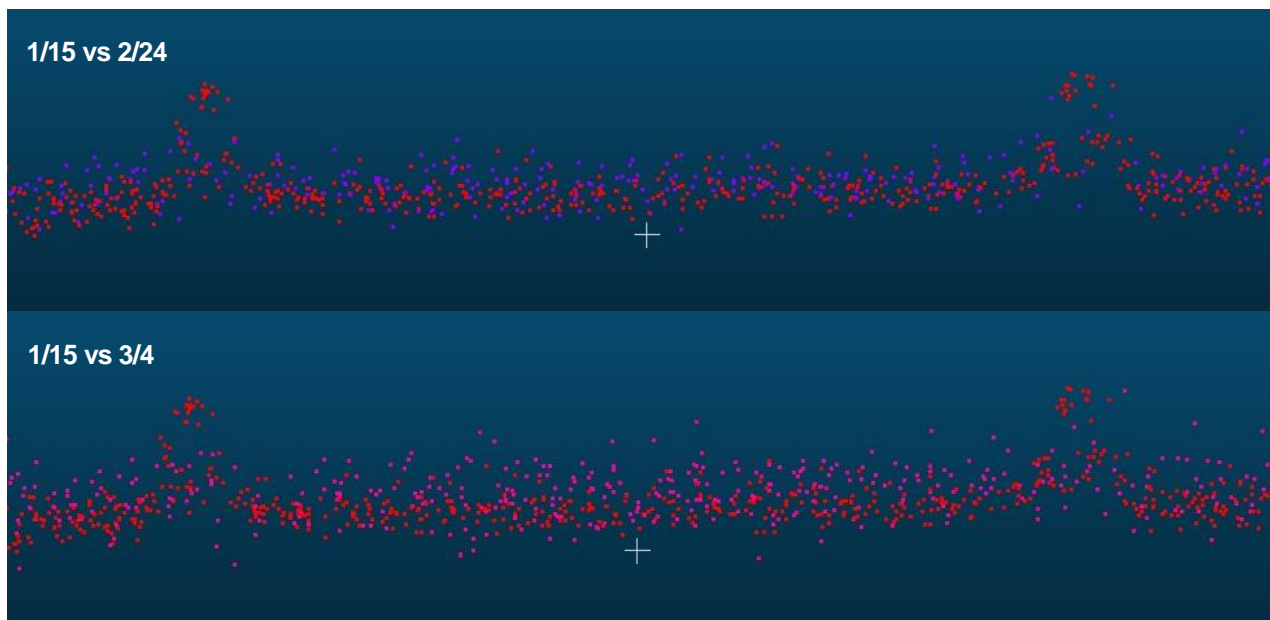


**Figure 30.** Profile detail of train tracks showing alignment between the 1/15 snow-off cloud (red) and the 2/24 and 3/4 snow-on clouds (violet and magenta).



**Figure 31.** Aerial photo of train tracks taken on 2/18 showing presence of snow on railroad ties. The elevation difference caused by this snow cover is observable in the 2/17 and 2/18 snow-on point clouds.



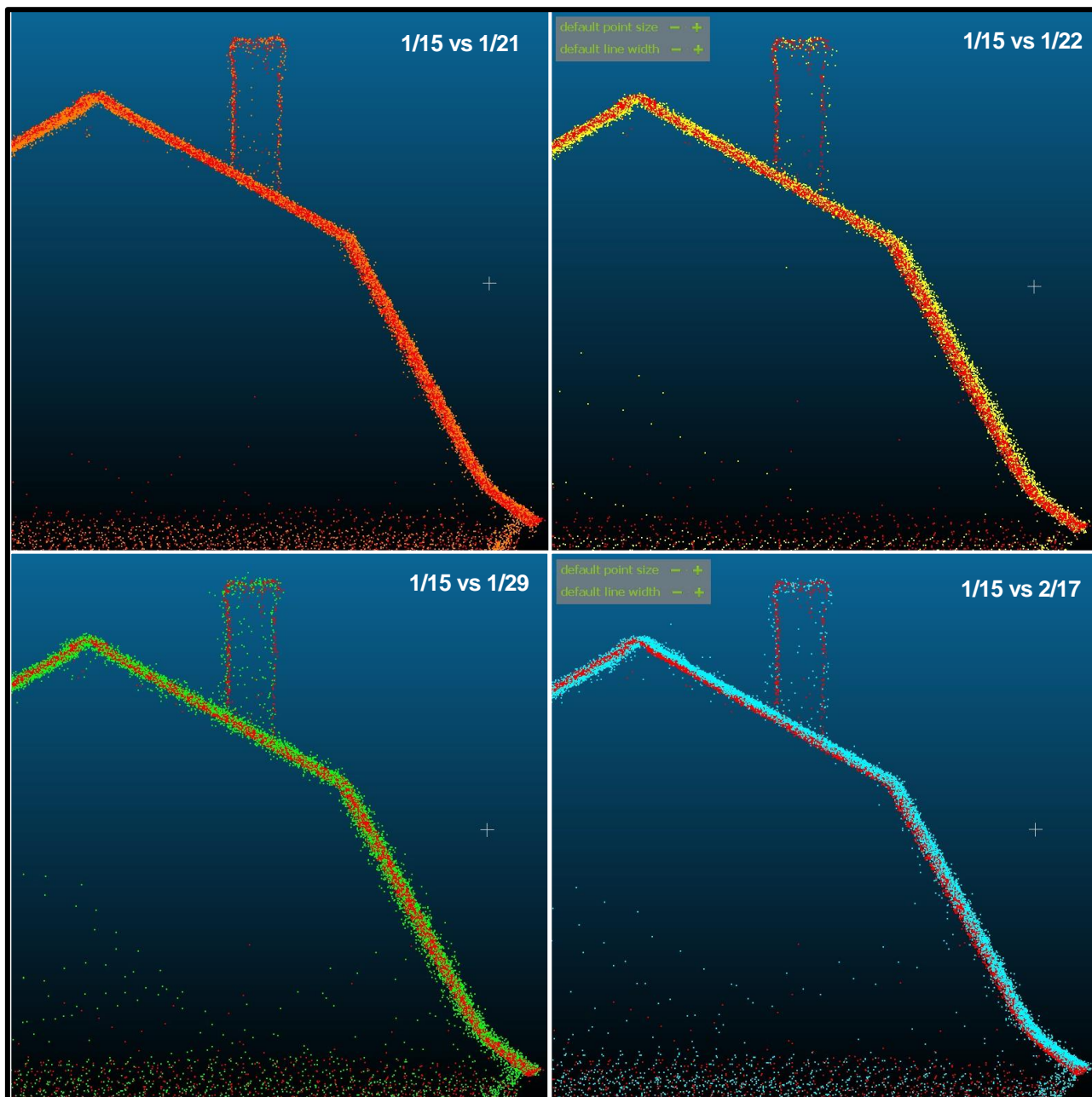


**Figure 32.** Profile detail of steep barn roof showing alignment between the 1/15 snow-off cloud (red) and the 1/21, 1/22, 1/29, and 2/17 (orange, yellow, green, and cyan).

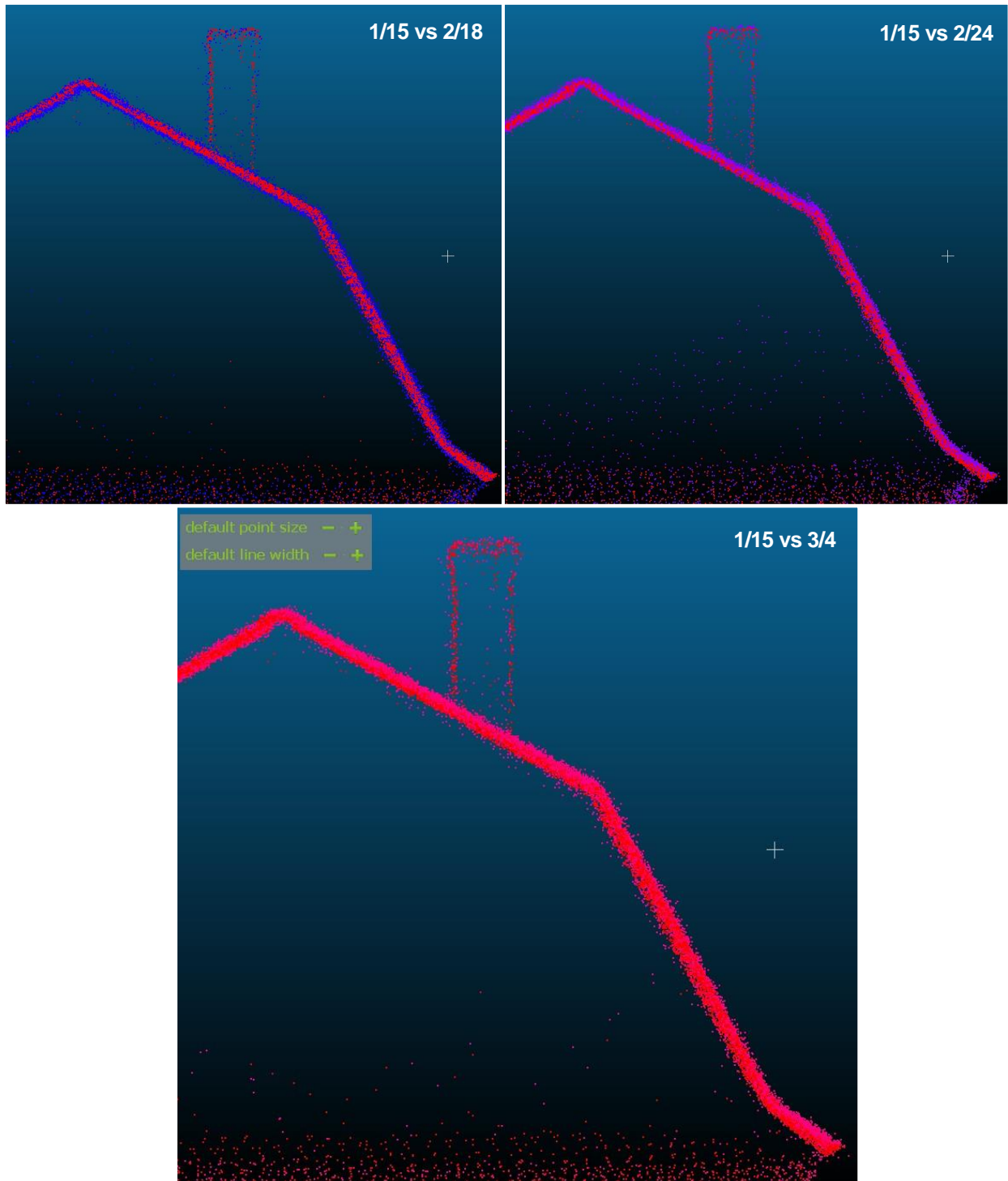


**Figure 33.** Profile detail of steep barn roof showing alignment between the 1/15 snow-off cloud (red) and the 2/18, 2/24, and 3/4 snow-on point clouds (blue, violet, and magenta).

Qualitative assessment also showed that point clouds very clearly showed variations in snow depth from cloud to cloud. This was especially evident where blowing snow piled up due to windbreaks or ditches. Examples are show in figures 34 and 35.

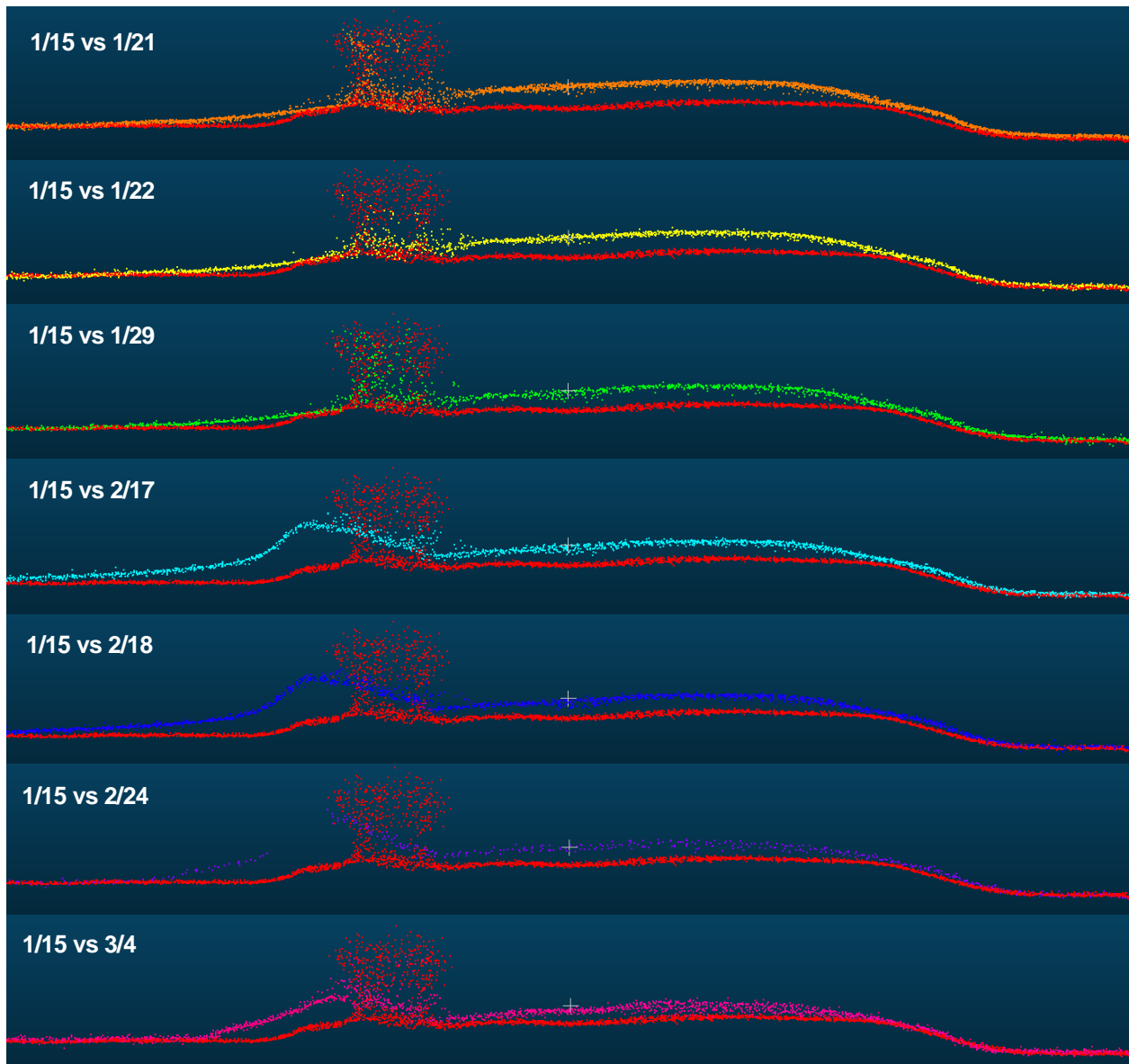


**Figure 34.** Profile detail of deep snowbank along N-S running vegetative windbreak. The 1/15 snow-off acquisition is displayed in red. The differences between the snow-off and each snow-on acquisition is evident in the point clouds.

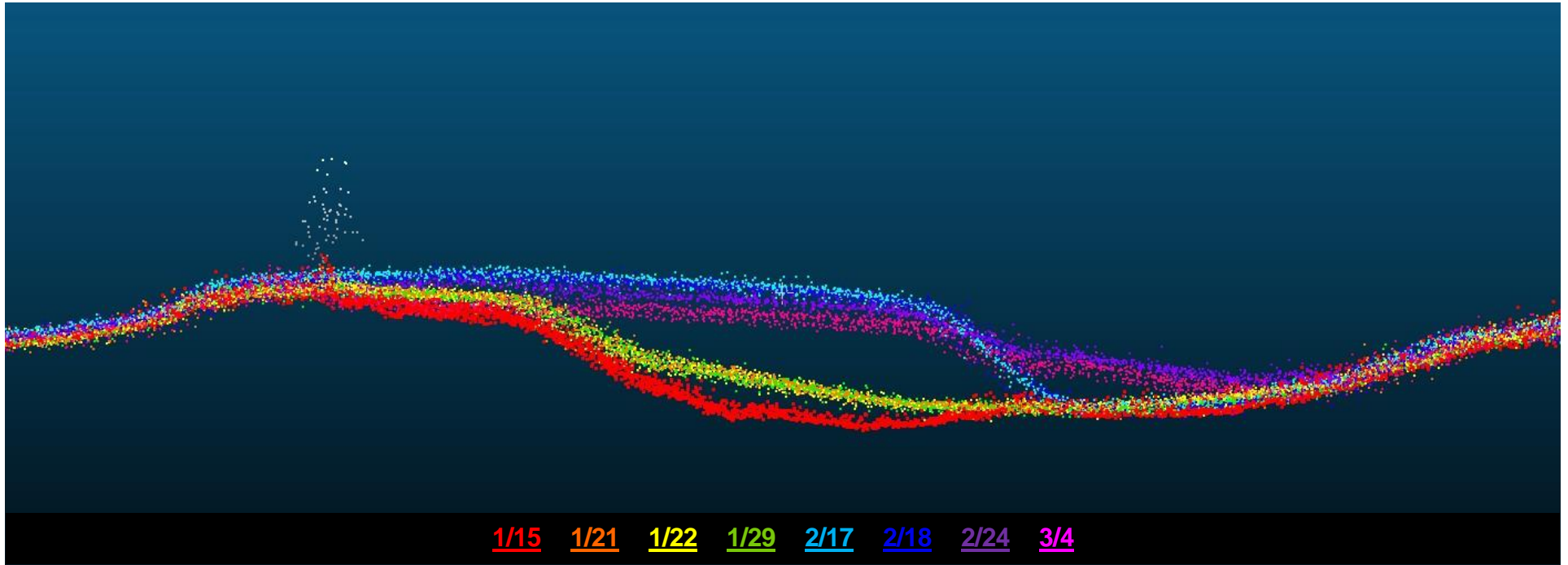


**Figure 35.** Profile detail of ditch running between fence (on left) and railroad tracks (out of shot on right). Snow depth variations can clearly be seen between point clouds from different acquisitions days.

Another important finding is the fact that snow surfaces appear to exist at the top of a point cloud's surface thickness, at least for 905nm LiDAR and the snow conditions present during our data acquisitions. This is different from the norm of the surface existing near the middle of the point cloud for other natural surfaces. Data users must take this fact into account when classifying snow surfaces. Additionally, we found that point clouds for areas containing a variety of snow coverage types (deep snow, thin snow, and bare areas) presented a unique challenge in obtaining an appropriate dz shift value for global accuracy. The location of the true surface inside the surface thickness varies for these different areas and normal ground extraction and shift methods do not yield optimal results. Alternative, more intensive steps must be taken to achieve DSMs with acceptable cloud-to-cloud alignment and global accuracy.

All point clouds achieved global accuracies and point densities meeting or exceeding USGS LBS QL1 and ASPRS Vertical Accuracy Class IV. The 1/15 snow-off and 3/4 snow-on clouds achieved USGS LBS QL0 and ASPRS Vertical Accuracy Class III. All clouds also achieved a minimum point density of 131.5 ppsm and surface point density (ground and model keypoints only) of 7.5 ppsm. The 0.10m value used for above and below tolerance in the model keypoints algorithm implies contours as tight as 0.20m can be accurately generated. The point clouds may support more detailed contours and data users may choose to experiment with extracting these at their own discretion. Information and statistics on each point cloud can be found in Tables 3 through 10 below.

1/15 Snow-Off		
Parameter	Value	
<b>General</b>		
Total Number of Points (all classes)	181,303,975	100%
Total Number of Ground Class Points	18,594,282	10.26%
Total Number of Model Keypoints	60,919	0.03%
Average Total Point Density Across Project (all classes)	181.3 ppsm	
Average Surface Point Density Across Project (ground + model keypoints)	18.7 ppsm	
<b>Truthing Information</b>		
Horizontal Project Data Units	Meters	
Vertical Project Data Units	Meters	
Elevation Delta Calculation Method	Interpolated from TIN surface	
LiDAR Classifications Included	Ground/Model Keypoints	
Quantity of Truthing Points Used for Vertical Shift	70	
Quantity of Truthing Points Used for Final Quality Check	16	
<b>Alignment Report (alignment relative to 1/15 Snow-off in select areas)</b>		
N/A	This is the snow-off cloud.	
<b>Global Quality Report</b>		
<i>Units of Meters</i>		
Average Vertical Error	- 0.003	
Maximum (highest) Vertical Error	+0.075	
Minimum (lowest) Vertical Error	- 0.057	
Average Magnitude Vertical Error	0.024	
Vertical Accuracy RMSE(z)	0.031	
Standard Deviation of Vertical Error	0.032	
NSSDA Vertical Accuracy at the 95% Confidence Level	0.062	
ASPRS Vertical Accuracy Class Achieved	III (<9.8cm NVA @ 95% CL, <14.7cm VVA @ 95% CL)	
USGS LBS Vertical Accuracy Class Achieved	QL0 (9.8cm NVA @ 95% CL, <15cm VVA @ 95% CL)	

Table 3. 1/15 snow-off final point cloud information and statistics.

1/21 Snow-On		
Parameter	Value	
<b>General</b>		
Total Number of Points (all classes)	224,064,678	100%
Total Number of Ground Class Points	16,369,047	7.3%
Total Number of Model Keypoints	65,255	0.03%
Average Total Point Density Across Project (all classes)	224.1 ppsm	
Average Surface Point Density Across Project (ground + model keypoints)	16.4 ppsm	
<b>Truthing Information</b>		
Horizontal Project Data Units	Meters	
Vertical Project Data Units	Meters	
Elevation Delta Calculation Method	Interpolated from TIN surface	
LiDAR Classifications Included	Ground/Model Keypoints	
Quantity of Points Used for Vertical Shift	14	
Quantity of Truthing Points Used for Final Quality Check	34	
<b>Alignment Report (alignment relative to 1/15 Snow-off in select areas, units of meters)</b>		
Average Vertical Error	0.000	
Maximum (highest) Vertical Error	0.104	
Minimum (lowest) Vertical Error	- 0.024	
Average Magnitude Vertical Error	0.019	
Vertical Accuracy RMSE(z)	0.031	
Standard Deviation of Vertical Error	0.032	
<b>Global Quality Report (units of meters)</b>		
Average Vertical Error	- 0.059	
Maximum (highest) Vertical Error	0.012	
Minimum (lowest) Vertical Error	- 0.127	
Average Magnitude Vertical Error	0.060	
Vertical Accuracy RMSE(z)	0.068	
Standard Deviation of Vertical Error	0.035	
NSSDA Vertical Accuracy at the 95% Confidence Level	0.133	
ASPRS Vertical Accuracy Class Achieved	IV (<19.6cm NVA @ 95% CL, <29.4cm VVA @ 95% CL)	
USGS LBS Vertical Accuracy Class Achieved	QL1 (<19.6cm NVA @ 95% CL, <30cm VVA @ 95% CL)	

Table 4. 1/21 snow-on final point cloud information and statistics.

1/22 Snow-On		
Parameter	Value	
<b>General</b>		
Total Number of Points (all classes)	114,016,206	100%
Total Number of Ground Class Points	9,558,712	8.38%
Total Number of Model Keypoints	56,721	0.05%
Average Total Point Density Across Project (all classes)	131.5 ppsm	
Average Surface Point Density Across Project (ground + model keypoints)	11.1 ppsm	
<b>Truthing Information</b>		
Horizontal Project Data Units	Meters	
Vertical Project Data Units	Meters	
Elevation Delta Calculation Method	Interpolated from TIN surface	
LiDAR Classifications Included	Ground/Model Keypoints	
Quantity of Points Used for Vertical Shift	14	
Quantity of Truthing Points Used for Final Quality Check	27	
<b>Alignment Report (alignment relative to 1/15 Snow-off in select areas, units of meters)</b>		
Average Vertical Error	- 0.002	
Maximum (highest) Vertical Error	0.105	
Minimum (lowest) Vertical Error	- 0.028	
Average Magnitude Vertical Error	- 0.002	
Vertical Accuracy RMSE(z)	0.031	
Standard Deviation of Vertical Error	0.032	
<b>Final Quality Report (units of meters)</b>		
Average Vertical Error	- 0.067	
Maximum (highest) Vertical Error	0.020	
Minimum (lowest) Vertical Error	- 0.155	
Average Magnitude Vertical Error	0.068	
Vertical Accuracy RMSE(z)	0.077	
Standard Deviation of Vertical Error	0.038	
NSSDA Vertical Accuracy at the 95% Confidence Level	0.150	
ASPRS Vertical Accuracy Class Achieved	IV (<19.6cm NVA @ 95% CL, <29.4cm VVA @ 95% CL)	
USGS LBS Vertical Accuracy Class Achieved	QL1 (<19.6cm NVA @ 95% CL, <30cm VVA @ 95% CL)	

Table 5. 1/22 snow-on final point cloud information and statistics.



1/29 Snow-On		
Parameter	Value	
<b>General</b>		
Total Number of Points (all classes)	157,153,029	100%
Total Number of Ground Class Points	11,150,768	7.10%
Total Number of Model Keypoints	64,426	0.04%
Average Total Point Density Across Project (all classes)	157.2 ppsm	
Average Surface Point Density Across Project (ground + model keypoints)	11.2 ppsm	
<b>Truthing Information</b>		
Horizontal Project Data Units	Meters	
Vertical Project Data Units	Meters	
Elevation Delta Calculation Method	Interpolated from TIN surface	
LiDAR Classifications Included	Ground/Model Keypoints	
Quantity of Points Used for Vertical Shift	14	
Quantity of Truthing Points Used for Final Quality Check	32	
<b>Alignment Report (alignment relative to 1/15 Snow-off in select areas, units of meters)</b>		
Average Vertical Error	0.000	
Maximum (highest) Vertical Error	0.093	
Minimum (lowest) Vertical Error	- 0.016	
Average Magnitude Vertical Error	0.016	
Vertical Accuracy RMSE(z)	0.027	
Standard Deviation of Vertical Error	0.028	
<b>Final Quality Report (units of meters)</b>		
Average Vertical Error	- 0.066	
Maximum (highest) Vertical Error	- 0.005	
Minimum (lowest) Vertical Error	- 0.143	
Average Magnitude Vertical Error	0.066	
Vertical Accuracy RMSE(z)	0.076	
Standard Deviation of Vertical Error	0.038	
NSSDA Vertical Accuracy at the 95% Confidence Level	0.149	
ASPRS Vertical Accuracy Class Achieved	IV (<19.6cm NVA @ 95% CL, <29.4cm VVA @ 95% CL)	
USGS LBS Vertical Accuracy Class Achieved	QL1 (<19.6cm NVA @ 95% CL, <30cm VVA @ 95% CL)	

**Table 6.** 1/29 snow-on final point cloud information and statistics.

2/17 Snow-On		
Parameter	Value	
<b>General</b>		
Total Number of Points (all classes)	142,636,050	100%
Total Number of Ground Class Points	9,220,013	6.46%
Total Number of Model Keypoints	69,798	0.05%
Average Total Point Density Across Project (all classes)	142.6 ppsm	
Average Surface Point Density Across Project (ground + model keypoints)	9.3 ppsm	
<b>Truthing Information</b>		
Horizontal Project Data Units	Meters	
Vertical Project Data Units	Meters	
Elevation Delta Calculation Method	Interpolated from TIN surface	
LiDAR Classifications Included	Ground/Model Keypoints	
Quantity of Points Used for Vertical Shift	14	
Quantity of Truthing Points Used for Final Quality Check	30	
<b>Alignment Report (alignment relative to 1/15 Snow-off in select areas, units of meters)</b>		
Average Vertical Error	- 0.022	
Maximum (highest) Vertical Error	0.102	
Minimum (lowest) Vertical Error	- 0.073	
Average Magnitude Vertical Error	0.043	
Vertical Accuracy RMSE(z)	0.051	
Standard Deviation of Vertical Error	0.047	
<b>Final Quality Report (units of meters)</b>		
Average Vertical Error	- 0.071	
Maximum (highest) Vertical Error	- 0.006	
Minimum (lowest) Vertical Error	- 0.155	
Average Magnitude Vertical Error	0.071	
Vertical Accuracy RMSE(z)	0.079	
Standard Deviation of Vertical Error	0.037	
NSSDA Vertical Accuracy at the 95% Confidence Level	0.156	
ASPRS Vertical Accuracy Class Achieved	IV (<19.6cm NVA @ 95% CL, <29.4cm VVA @ 95% CL)	
USGS LBS Vertical Accuracy Class Achieved	QL1 (<19.6cm NVA @ 95% CL, <30cm VVA @ 95% CL)	

Table 7. 2/17 snow-on final point cloud information and statistics.

2/18 Snow-On		
Parameter	Value	
<b>General</b>		
Total Number of Points (all classes)	151,246,744	100%
Total Number of Ground Class Points	9,980,115	6.60%
Total Number of Model Keypoints	70,875	0.05%
Average Total Point Density Across Project (all classes)	151.2 ppsm	
Average Surface Point Density Across Project (ground + model keypoints)	10.1 ppsm	
<b>Truthing Information</b>		
Horizontal Project Data Units	Meters	
Vertical Project Data Units	Meters	
Elevation Delta Calculation Method	Interpolated from TIN surface	
LiDAR Classifications Included	Ground/Model Keypoints	
Quantity of Points Used for Vertical Shift	14	
Quantity of Truthing Points Used for Final Quality Check	31	
<b>Alignment Report (alignment relative to 1/15 Snow-off in select areas, units of meters)</b>		
Average Vertical Error	- 0.001	
Maximum (highest) Vertical Error	0.136	
Minimum (lowest) Vertical Error	- 0.035	
Average Magnitude Vertical Error	0.027	
Vertical Accuracy RMSE(z)	0.042	
Standard Deviation of Vertical Error	0.044	
<b>Final Quality Report (units of meters)</b>		
Average Vertical Error	- 0.088	
Maximum (highest) Vertical Error	- 0.030	
Minimum (lowest) Vertical Error	- 0.139	
Average Magnitude Vertical Error	0.088	
Vertical Accuracy RMSE(z)	0.092	
Standard Deviation of Vertical Error	0.029	
NSSDA Vertical Accuracy at the 95% Confidence Level	0.181	
ASPRS Vertical Accuracy Class Achieved	IV (<19.6cm NVA @ 95% CL, <29.4cm VVA @ 95% CL)	
USGS LBS Vertical Accuracy Class Achieved	QL1 (<19.6cm NVA @ 95% CL, <30cm VVA @ 95% CL)	

Table 8. 2/18 snow-on final point cloud information and statistics.

2/24 Snow-On		
Parameter	Value	
<b>General</b>		
Total Number of Points (all classes)	117,312,461	100%
Total Number of Ground Points	6,382,063	5.44%
Total Number of Model Keypoints	60,963	0.05%
Average Total Point Density Across Project (all classes)	136.0 ppsm	
Average Surface Point Density Across Project (ground + model keypoints)	7.5 ppsm	
<b>Truthing Information</b>		
Horizontal Project Data Units	Meters	
Vertical Project Data Units	Meters	
Elevation Delta Calculation Method	Interpolated from TIN surface	
LiDAR Classifications Included	Ground/Model Keypoints	
Quantity of Truthing Points Used for Vertical Shift	14	
Quantity of Truthing Points Used for Final Quality Check	27	
<b>Alignment Report (alignment relative to 1/15 Snow-off in select areas, units of meters)</b>		
Average Vertical Error	- 0.011	
Maximum (highest) Vertical Error	0.058	
Minimum (lowest) Vertical Error	- 0.032	
Average Magnitude Vertical Error	0.019	
Vertical Accuracy RMSE(z)	0.024	
Standard Deviation of Vertical Error	0.022	
<b>Final Quality Report (units of meters)</b>		
Average Vertical Error	- 0.055	
Maximum (highest) Vertical Error	0.003	
Minimum (lowest) Vertical Error	- 0.124	
Average Magnitude Vertical Error	0.055	
Vertical Accuracy RMSE(z)	0.063	
Standard Deviation of Vertical Error	0.032	
NSSDA Vertical Accuracy at the 95% Confidence Level	0.124	
ASPRS Vertical Accuracy Class Achieved	IV (<19.6cm NVA @ 95% CL, <29.4cm VVA @ 95% CL)	
USGS LBS Vertical Accuracy Class Achieved	QL1 (<19.6cm NVA @ 95% CL, <30cm VVA @ 95% CL)	

Table 9. 2/24 snow-on final point cloud information and statistics.

3/4 Snow-On		
Parameter	Value	
<b>General</b>		
Total Number of Points (all classes)	146,417,527	100%
Total Number of Ground Points	9,188,018	6.28%
Total Number of Model Keypoints	63,517	0.04%
Average Total Point Density Across Project (all classes)	146.4 ppsm	
Average Surface Point Density Across Project (ground + model keypoints)	9.3 ppsm	
<b>Truthing Information</b>		
Horizontal Project Data Units	Meters	
Vertical Project Data Units	Meters	
Elevation Delta Calculation Method	Interpolated from TIN surface	
LiDAR Classifications Included	Ground/Model Keypoints	
Quantity of Truthing Points Used for Vertical Shift	14	
Quantity of Truthing Points Used for Final Quality Check	39	
<b>Alignment Report (alignment relative to 1/15 Snow-off in select areas, units of meters)</b>		
Average Vertical Error	- 0.001	
Maximum (highest) Vertical Error	0.052	
Minimum (lowest) Vertical Error	- 0.024	
Average Magnitude Vertical Error	0.012	
Vertical Accuracy RMSE(z)	0.018	
Standard Deviation of Vertical Error	0.018	
<b>Final Quality Report (units of meters)</b>		
Average Vertical Error	- 0.009	
Maximum (highest) Vertical Error	0.107	
Minimum (lowest) Vertical Error	- 0.081	
Average Magnitude Vertical Error	0.031	
Vertical Accuracy RMSE(z)	0.039	
Standard Deviation of Vertical Error	0.039	
NSSDA Vertical Accuracy at the 95% Confidence Level	0.077	
ASPRS Vertical Accuracy Class Achieved	III (<9.8cm NVA @ 95% CL, <14.7cm VVA @ 95% CL)	
USGS LBS Vertical Accuracy Class Achieved	QL0 (9.8cm NVA @ 95% CL, <15cm VVA @ 95% CL)	

Table 10. 3/4 snow-on final point cloud information and statistics.

### 1550nm LiDAR Snow Surface Mapping

The snow-on 1550nm test acquisition performed on 1/29 showed that 1550nm LiDAR does not work well on snow surfaces. While returns were recorded, the resulting point cloud contained large quantities of noise making it difficult to rectify point cloud swathes from different flight lines and obtain a useable unified point cloud. The point cloud also displayed a very large surface thickness, which would have made accurate classification much more difficult. Additionally, there were large areas with very few or no returns at all, resulting in gaps in the point cloud, which would have, in turn, resulted in gaps in the DSM. The results of the efficacy test clearly showed that 905nm LiDAR is superior for snow surface mapping compared to 1550nm.

### LiDAR Surface Accuracy on Ice

Five GNSS truthing points collected on ice surfaces on 3/4 were compared to the 3/4 DSM. Results of the comparison show that the 905nm LiDAR system used could yield accurate results for ice surface mapping. Table 11 shows the points, dz values, and statistics for the five ice surface points.

Point ID	Northing	Easting	GNSS Z	LiDAR Z	dz
4042	5212650.033	579969.679	1289.683	1289.594	- 0.089
4037	5212050.971	579914.853	1292.754	1292.760	0.006
4040	5212351.601	579948.395	1290.709	1290.687	- 0.022
4041	5212345.542	579947.012	1290.713	1290.657	- 0.056
4044	5212886.288	579192.306	1293.755	1293.716	- 0.039
Average Vertical Error			<b>- 0.040</b>		
Maximum (highest) Vertical Error			<b>- 0.089</b>		
Minimum (lowest) Vertical Error			<b>0.006</b>		
Average Magnitude Vertical Error			<b>0.042</b>		
Vertical Accuracy RMSE(z)			<b>0.051</b>		
Standard Deviation of Vertical Error			<b>0.036</b>		

**Table 11.** GNSS ice surface truthing points and resulting statistics from a comparison run between these points and the 3/4 LiDAR DSM.

Vertical error statistics for this comparison show good agreement between the GNSS ice surface points and the 3/4 LiDAR DSM. This indicates that a 905nm LiDAR system could yield accurate surface mapping data for ice surfaces. More extensive data obtained through an experiment designed to investigate this application would be needed for more conclusive results.